# The Diel and Seasonal Heterogeneity of Carbonate Chemistry and Dissolved Oxygen in Three Types of Macroalgal Habitats

Huiru Li[1†], Hanbi Moon[1,2†], Eun Ju Kang[1], Ja-Myung Kim[3], Miok Kim[3], Kitack Lee[3], Cheol-Woo Kwak[4], Haryun Kim[2], Il-Nam Kim[5], Ki Yeol Park[6], Young Kweon Lee[6], Ji Woong Jin[6], Matthew S. Edwards[7] and Ju-Hyoung Kim[1*]

[1] Department of Aquaculture and Aquatic Science, Kunsan National University, Gunsan, South Korea, [2] East Sea Research Institute, Korea Institute of Ocean Science & Technology, Uljin, South Korea, [3] Division of Environmental Science and Engineering, Pohang University of Science & Technology, Pohang, South Korea, [4] Korea Marine Environment & Ecology Research Institute, Bucheon, South Korea, [5] Department of Marine Science, Incheon National University, Incheon, South Korea, [6] Ecological Restoration Division, Korea Fisheries Resources Agency (East Sea Branch), Pohang, South Korea, [7] Department of Biology, San Diego State University, San Diego, CA, United States

As concerns about ocean acidification continue to grow, the importance of macroalgal communities in buffering coastal seawater biogeochemistry through their metabolisms is gaining more attention. However, studies on diel and seasonal fluctuations in seawater chemistry within these communities are still rare. Here, we characterized the spatial and temporal heterogeneity in diel and seasonal dynamics of seawater carbonate chemistry and dissolved oxygen (DO) in three types of macroalgal habitats (UAM: ulvoid algal mat dominated, TAM: turf algal mat dominated, and SC: *Sargassum horneri* and coralline algae dominated). Our results show that diel fluctuations in carbonate parameters and DO varied significantly among habitat types and seasons due to differences in their biological metabolisms (photosynthesis and calcification) and each site's hydrological characteristics. Specifically, carbonate parameters were most affected by biological metabolisms at the SC site, and by environmental variables at the UAM site. Also, we demonstrate that macroalgal communities reduced ocean acidification conditions when ocean temperatures supported photosynthesis and thereby the absorption of dissolved inorganic carbon. However, once temperatures exceeded the optimum ranges for macroalgae, respiration within these communities exceeded photosynthesis and increased $CO_2$ concentrations, thereby exacerbating ocean acidification conditions. We conclude that the seawater carbonate chemistry is strongly influenced by the metabolisms of the dominant macroalgae within these different habitat types, which may, in turn, alter their buffering capacity against ocean acidification.

**Keywords: biogeochemical interaction, carbonate chemistry, dissolved oxygen, diel fluctuation, macroalgal habitat**

# INTRODUCTION

Macroalgae provide numerous ecological functions such as enhancing the primary production and providing food and shelter for other organisms (Kim et al., 2015; Mineur et al., 2015; Metzger et al., 2019; Edwards et al., 2020; Sullaway and Edwards, 2020). With increasing impacts of ocean acidification (OA) on marine ecosystems (Doney et al., 2009; IPCC, 2019), the role of macroalgae, and more specifically their metabolisms, in buffering coastal ecosystems against OA has received considerable attention because they can alter seawater carbonate parameters through photosynthesis and respiration, and to a lesser extent calcification and dissolution (Comeau and Cornwall, 2016). Indeed, macroalgae can reduce seawater $pCO_2$ within some coastal waters, and thereby temporarily mitigate the effects of OA (Murie and Bourdeau, 2020; Xiao et al., 2021). They can also influence diel and seasonal cycles in seawater chemistry because their metabolisms are strongly influenced by patterns of solar irradiance. These cycles, however, likely also vary among habitats that are characterized by different macroalgae with different metabolisms. As a result, examining diel and seasonal variations in seawater chemistry within and around different types of macroalgal communities can help discern the importance of biological and chemical interactions between macroalgae and seawater chemistry parameters (Gonzales et al., 2017; Carrano et al., 2020; Carrano et al., 2021).

The coastal ocean experiences large fluctuations in its carbonate chemistry due to both hydrodynamic and biological activities (Lee et al., 2011; Cai et al., 2020; Kim et al., 2020b). In fact, variability in seawater pH within some coastal oceans can be greater than that in the open ocean (Hofmann et al., 2011). Several studies have shown that substantial diel fluctuations in pH and $pCO_2$ occur in the waters around macroalgal communities (e.g., Delille et al., 2000; Middelboe and Hansen, 2007; Delille et al., 2009; Krause-Jensen et al., 2015). In general, photosynthesis and respiration strongly contribute to diel variations in inorganic carbon by absorbing $CO_2$ during the day and releasing $CO_2$ at night (Chou et al., 2018), with the net effects of these being manifested in net community production (NCP) (Cyronak et al., 2018; Edwards et al., 2020). To a lesser extent, the production and dissolution of $CaCO_3$ by calcifying organisms (e.g., coralline algae, epiphytes and benthic invertebrates) also alter seawater carbonate chemistry, with the net effects of these being quantified as net community calcification (NCC) (Turk et al., 2015; Ragazzola et al., 2021). Both NCP and NCC can regulate seawater total alkalinity ($A_T$) and total dissolved inorganic carbon ($C_T$) following a well-established stoichiometry, where the ratio of $A_T$-$C_T$ for NCP is –0.2 and the ratio for NCC is 2.0 (Krumins et al., 2013; Sippo et al., 2016). Hence, measuring the relationship between $A_T$ and $C_T$ could be an effective way to identify the dominant metabolism within these communities. For example, while NCP is the dominant metabolism within some shallow coastal regions of the Mediterranean Sea throughout the year, NCC can lead to decreases in $A_T$ during the summer within areas of the coast that are dominated by coralline algae whose metabolisms alter $\Delta A_T$/

$\Delta C_T$ ratios (Ragazzola et al., 2021). Another potential metric for evaluating the biogeochemical effects of macroalgal communities on seawater chemistry is the relationship between $CO_2$ partial pressure ($pCO_2$) and dissolved oxygen (DO), as photosynthesis lowers $pCO_2$ but increases DO, while respiration releases $CO_2$ but consumes DO (Zhai et al., 2009; Vachon et al., 2020). Hence, the coupling $pCO_2$ and DO can help discern the status of ocean metabolism, explicitly the ratio of primary production and respiration (Kuss et al., 2006; Zhai and Dai, 2009; Vachon et al., 2020).

At present, the ability of macroalgae to mitigate OA by altering seawater chemistry has been studied in kelp beds (Frieder et al., 2012; Britton et al., 2016; Pfister et al., 2019; Edwards et al., 2020) and seaweed farms (Li et al., 2021; Xiao et al., 2021). In contrast, other macroalgal communities in coastal oceans have seldom been studied (Middelboe and Hansen, 2007; Wahl et al., 2018). The types of macroalgal communities are diverse, and their influence on the biogeochemical interactions within the surrounding environment can vary depending on their community structures (Kim et al., 2015; Spector and Edwards, 2020). For example, in habitats dominated by opportunistic macroalgae, fluctuations in biogeochemical parameters may be large because of high rates of photosynthesis and respiration, whereas at the same time the absence of calcifying organisms may result in only small changes in $A_T$ (e.g., Deng et al., 2018). On the other hand, habitats dominated by canopy-forming macroalgae such as kelp beds exhibit high rates of respiration due to their strong ability to capture organic matter (Edwards et al., 2020; Spector and Edwards, 2020). However, the coralline algae that inhabit the rocky bottom within these kelp beds can create unexpected biogeochemical responses because of their integrated metabolisms (Edwards et al., 2020). In the turf algal mats, lower metabolism appears than that in the blooming area of the canopies, but more complex variations in $A_T$ and $C_T$ occur in the turf algae because of the higher species diversity. However, studies on the ability of different macroalgal communities to alter seawater carbonate parameters have not been conducted. In particular, it is necessary to better understand diel fluctuations in carbonate parameters within these communities because changes in these parameters can reveal the influence of their biological metabolisms, which are regulated by changes in irradiance between the daytime and nighttime.

Anthropogenic activities are leading to widespread changes in macroalgal communities along the temperate coast of Korea, and acclimation patterns of the dominant macrophytes (i.e., their phenology) are clearly observed according to the seasons. For example, in Pohang new port, Korea, coralline algae are dominant in all seasons, but the canopy-forming alga, *Sargassum horneri* is abundant only in winter (Yoo et al., 2006). Indeed, total macroalgal biomass is high in winter and spring, and low in summer and autumn. In addition, opportunistic macroalgae have become abundant in coastal areas with intensive nutrient inputs (Lee and Kang, 2020; Kim et al., 2020b; Kang et al., 2021), while coralline algae have become dominant in other areas because of climate change and increased herbivore pressure on fleshy macroalgae (Kim et al., 2020a). Over
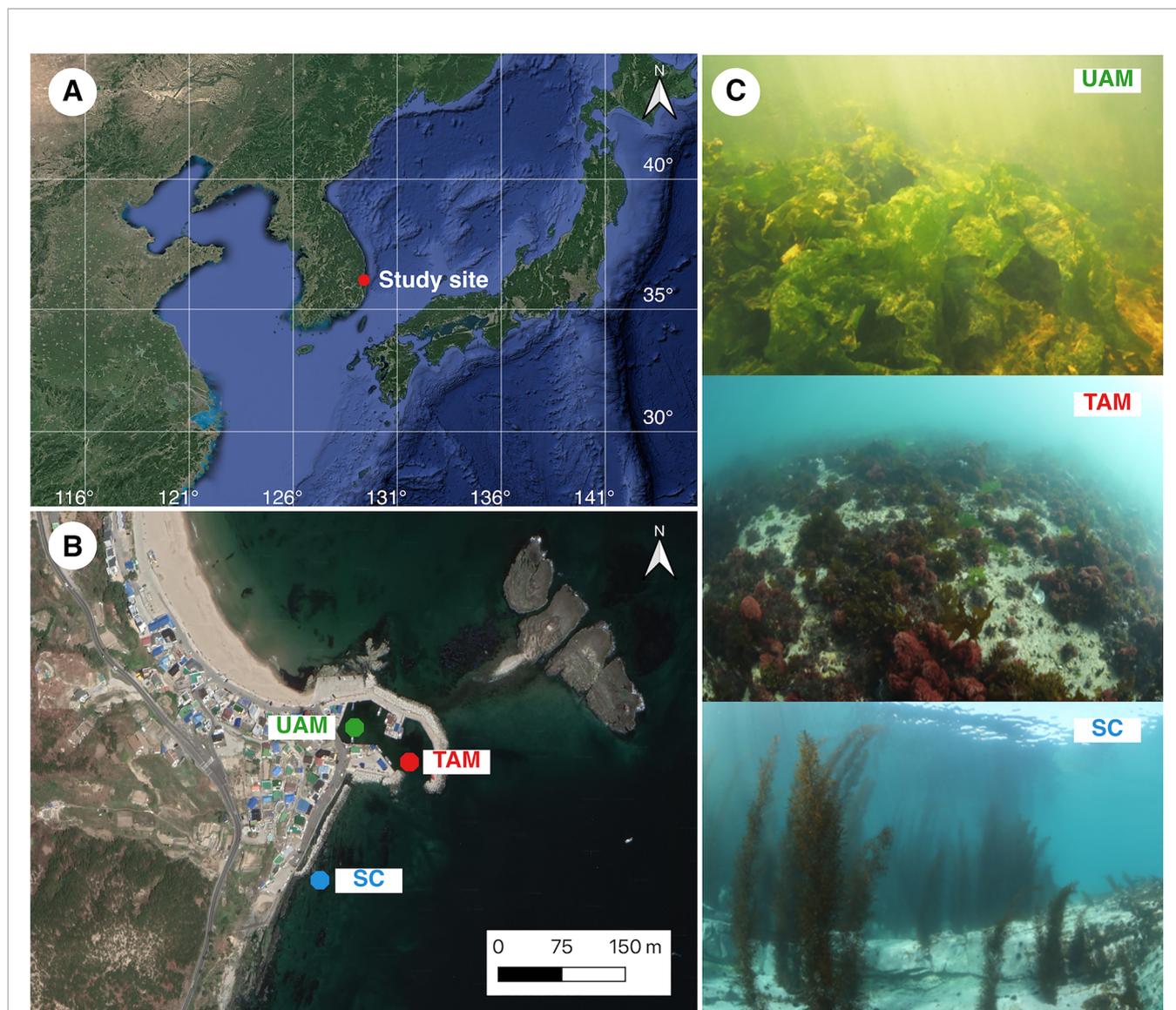
**FIGURE 1 | (A)** The location of study area where the three sites with different macroalgal habitats were located in Odo beach of Pohang on the east coast of the Korea peninsula, **(B)** locations of the three study sites with different macroalgal habitats (UAM, ulvoid algal mat; TAM, turf algal mat; SC, coexisting *Sargassum horneri* and crustose coralline algae) and **(C)** photographs of three macroalgal habitats (UAM: top, TAM: mid, and SC: bottom). Maps were generated using a Google satellite map and QGIS 3.20 Odense software (QGIS Development Team, 2021).

time, these macroalgal communities are turning into tiny mosaics with strong spatial heterogeneity. Hence, it is important to investigate fluctuations in seawater chemistry in and around these different communities throughout the year if we are to evaluate seasonal variation in their abilities to buffer against changes in pH (Delille et al., 2009; Koweek et al., 2017). In this study, we investigate diel and seasonal heterogeneity in carbonate chemistry and dissolved oxygen within different macroalgal habitats, and attempt to understand how diel metabolic activities within various macroalgal habitats are affecting seawater chemistry in different seasons, and their implications for OA mitigation.

## MATERIALS AND METHODS

### Study Area

Seawater carbonate parameters and DO were measured in three macroalgal habitats along the east coast of the Korean peninsula near the Odo, Heunghae-eup, Pohang-si (36°9'15''N, 129°24'3''E) (**Figure 1**). This area is located in the East Sea (a marginal sea in the northwestern Pacific), which takes up substantial amounts of anthropogenic $CO_2$ that subsequently changes the carbonate chemistry of the East Sea (Park et al., 2006). Otherwise, the study area has no large-scale sources of pollutants, with the only sewage flowing from nearby villages

(Heunghae-eup: with a population of less than 40,000) and harbors. The water mass at the sampling area is physically quite stable. Specifically, the tidal range is less than 30 cm, and there are nearly no tidal currents. In addition, depending on the weather conditions, the mixing of seawater occurs actively by waves from the open ocean. Our previous study showed that the concentrations of nitrate and phosphate were maintained at relatively low and stable levels, up to 12 µmol kg$^{-1}$ and 1 µmol kg$^{-1}$ respectively (Unpublished data). Three macroalgal habitats were chosen within the study area as sampling sites, namely ulvoid algal mats (UAM), turf algal mats (TAM), and a coexisting habitat of the canopy-forming macroalga, *Sargassum horneri*, and crustose coralline algae (SC). Specifically, the UAM site, which covers approximately 2,500 m$^2$, is located inside of the harbor where the sewage from villages is input directly and ulvoid green algae (e.g., *Ulva australis*) are predominant, showing close to 100% coverage. Also, small individuals of *Undaria pinnatifida* are attached to the harbor's concrete wall. Metabolism at the UAM site is expected to be dominated by photosynthesis/respiration of ulvoid seaweed and microalgae, and by microbial respiration. The TAM site, which covers approximately 3,550 m$^2$, is located near the outer harbor and has more than 30 species of understory and canopy-forming macrophytes that are distributed haphazardly (e.g., **Chlorophyta**: *Ulva* spp., **Phaeophyta:** *S. horneri, Saccharina japonica, U. pinnatifida*; **Rhodophyta**: *Portieria japonica, Callophyllis japonica, Plocamium telfairiae*; **Vascular plants**: *Zostera marina, Phyllospadix iwatensis*, etc.). Since the exchange of seawater at the TAM site is relatively active compared to the UAM site, photosynthesis and respiration by the benthic community are balanced, and microbial respiration is expected to be relatively low. The SC site, which is connected to an open ocean and not semi-enclosed, is located at the outside of the harbor and is a transitional habitat to an urchin barren ground where most of the foliose macroalgae have disappeared, except for *S. horneri*, and where the crustose coralline algae (CCA) species have become dominant due to the intense herbivore pressure. At the SC site, we can expect intense photosynthesis/respiration by *S. horneri* and CCA, and calcification/dissolution by CCA. Also, the biomass of benthic macrofauna was less than 16% compared to that of macroalgae near the TAM and SC sites (see **Supplementary Tables S1**, **S2**). The distance between three sampling sites is very close (UAM to SC: 310 m; UAM to TAM: 120 m; TAM to SC: 270 m). Salinity (during the carbonate chemistry analysis) and temperature data (during the *in-situ* monitoring) are presented in **Supplementary Table S3**.

## Seawater Sampling and Determination of Carbonate Parameters ($nA_T$, $nC_T$, and $n$pH$_T$)

To characterize diel fluctuations in seawater carbonate parameters, seawater was collected from each of the three macroalgal habitats (UAM, TAM, and SC) during four seasonal events in 2019: winter (from Feb. 12 at 9:00 AM to Feb. 13 at 7:00 AM), spring (from May 30 at 9:00 AM to May 31 at 6:00 AM), summer (from Aug. 8 at 9:00 AM to Aug. 9 at 6:00 AM), and autumn (from Oct. 10 at 9:00 AM to Oct. 11 at 6:00

AM). At each site, seawater was collected every 2 to 3 hours over a 24-hour period to determine total alkalinity ($A_T$), total inorganic carbon ($C_T$), and pH on the total hydrogen ion concentration scale (total scale, pH$_T$). As three sites were close to each other, we collected the samples for each site at similar times on the same day. All seawater sampling procedures and carbonate chemistry analyses followed the standard operation procedures for ocean $CO_2$ measurement as described by Dickson et al. (2007). The seawater samples were collected from about 0.5 m above the bottom of macroalgal habitats using a custom-made sampler (2 L capacity) made of transparent PC material, and quickly transferred to two 500 ml borosilicate airtight glass bottles respectively (1,500-500 Pyrex; Corning, NY, USA) without introducing air bubbles. The bottles were immediately closed with vacuum grease (Apiezon M grease; M&I Materials Ltd., Manchester, UK) after adding 100 µL saturated mercuric chloride ($HgCl_2$) to poison all organisms and stop the metabolism. These bottles were then stored cold in the dark until measurement.

Seawater $A_T$, $C_T$, and pH$_T$ were measured within two weeks after sampling. Concentrations of $A_T$ and $C_T$ were measured using potentiometric and coulometric titration methods, respectively, within the VINDTA system (Versatile Instrument for the Determination of Titration Alkalinity, Marianda, Kiel, Germany). For $A_T$ measurements, the samples were titrated with weak HCl (0.2 M). The volume of added acid was recorded at least 25 points until the titration to the endpoint [Electromotive force (EMF) ≈ 400 mV]. The values of $A_T$ were determined from the resulting titration data using a non-linear curve fitting within the VINDTA LabView-software (Millero et al., 1993; Dickson et al., 2007). Note that $A_T$ errors associated with organic acids and particulate organic matter were found to be negligible in this environment (Ko et al., 2016; Lee et al., 2021). To analyze $C_T$, the coulometer cell was filled with ethanol amine and a colorimetric indicator. When the gas stream passes through the solution, $CO_2$ is absorbed quantitatively. Seawater pH$_T$ was determined spectrophotometrically (Clayton and Byrne, 1993) by adding the sulfonephthalein indicator m-Cresol Purple (mCP, Sigma-Aldrich Chemical Co., St. Louis, MO, USA) at the room temperature of 25°C. The absorbances of samples with and without the mCP indicator were measured using a 10 cm path length cuvette and a spectrophotometer (Agilent 8453 UV-Visible Spectrophotometer; Agilent Technologies, Pal Alto, CA, USA) at wavelengths of 730, 578, and 434 nm (Clayton and Byrne, 1993; Dickson, 1993). Specifically, the tube and cuvette were rinsed with sample before each measurement, and then the cuvette full of sample was placed in the sample compartment of the spectrophotometer. After the absorbance measurement, 80 µl mCP indicator was injected into the cuvette and mixed with sample by gently inverting. Then the cuvette was returned to the spectrophotometer to measure again the absorbances of the sample with indicator. Prior to measurements, the precision and performance of the instruments were verified using certified reference materials (CRMs, supplied by A. G. Dickson, Scripps Institute of Oceanography, U.S.A., batch number 180, 183 and 184). The accuracy of these measurements was ± 1.5 µmol kg$^{-1}$ for

$A_T$, ± 2 µmol kg$^{-1}$ for $C_T$ and ± 0.004 unit for pH$_T$. The salinity of samples was measured using a salinometer (Portasal$^{TM}$ 8410A; Guideline Instruments Ltd., USA). To consider only the effects of biological metabolism on the carbonate chemistry, the values of $A_T$ and $C_T$ were normalized to salinity (by multiplying by a factor of the averaged salinity value/$S$, where $S$ is the measured salinity value of each sample) to remove the effect of salinity variations on $A_T$ and $C_T$. Also, values of pH$_T$ were normalized to temperature of 25°C to remove the effect of temperature on pH$_T$. The normalized values are expressed as $nA_T$, $nC_T$, $n$pH$_T$ hereafter.

## *In-Situ* Monitoring Seawater Biogeochemical Parameters ($p$CO$_2$, DO, and pH$_{NIST}$)

Various data logger sensors were deployed at each of the three macroalgal habitats to monitor *in-situ* seawater biogeochemical parameters, including partial pressure of carbon dioxide ($p$CO$_2$), dissolved oxygen (DO) and pH on the scale of National Institute of Standards and Technology (NIST scale, pH$_{NIST}$) for two to six days each in winter (from Feb. 18 to Apr. 2), spring (from May 24 to Jun. 3), summer (from Aug. 9 to 19), and autumn (from Oct. 15 to 23) in 2019. The *in-situ* measurements at three sites were conducted on different dates during the monitoring period since we needed to put the sensors at one site after another. The number of monitoring days at each site was different, from at least two to six days, because of the weather and other practical considerations. In particular, the UAM site was monitored for only 34 hours in summer due to the interruption by a typhoon. Although the winter monitoring continued until Apr. 2 (spring), these data were included in winter data because there was no significant change in water temperature during monitoring (approximately 11°C). A CONTROS HydroC CO$_2$ sensor (Kongsberg Maritime Contros GmbH, Kiel, Germany) equipped with a non-dispersive infrared (NDIR) analyzer was used to measure $p$CO$_2$, and data were stored every 1 hour. This instrument and 16.8V lithium battery were fixed together on a stainless-steel frame and placed at 0.2 m above the bottom of each macroalgal habitat. A HOBO datalogger U26-001 and a HOBO datalogger MX2501 (onset computer corporation, Bourne, MA, USA) were used to monitor DO and pH$_{NIST}$ with temperature respectively, which were fastened on a stainless-steel frame and deposited at 0.2 m above the bottom of each macroalgal habitat. The caps of DO dataloggers were replaced every six months to obtain reliable results. Before the *in-situ* pH monitoring, dataloggers were calibrated using the NIST standard reference buffer (pH 4.0, 7.0, and 10.0; YSI 3821~3823, YSI Inc./ Xylem Inc., USA). After *in-situ* monitoring, pH$_{NIST}$ values showed stable signal when re-calibration with the reference buffer. Data of DO and pH$_{NIST}$ were stored every 10 minutes.

## Data Analysis

Statistical analyses were performed using SPSS software version 25, and PRIMER/PERMANOVA version 6.1.13. All data were checked for normality and equality of variances prior to testing. Data for normalized carbonate chemistry ($nA_T$, $nC_T$, and $n$pH$_T$), and *in-situ* monitoring data ($p$CO$_2$, DO, and pH$_{NIST}$) were all non-normal and heteroscedastic, and could not be fixed by transformation.

Therefore, differences in each parameter among seasons and macroalgal sites were analyzed with separate two-way Model I PERMANOVAs on Euclidean distance-based resemblance matrices, as described by Anderson and Walsh (2013). Data were square root transformed prior to analyses. Due to very large sample sizes (100's to 1,000's depending on variable), our analyses had an abundance of statistical power to resolve even very small differences in our response variables. Consequently, we acknowledge *p*-values alone may not be entirely informative when evaluating the effects of each explanatory factor, as described for ANOVA by Graham and Edwards (2001). We therefore include the amount of variation in our response variables (% of total) that was explained by each explanatory factor by calculating their magnitudes of effect ($\omega^2$) (Graham and Edwards, 2001). Following this, *a priori* hypotheses regarding general differences among the four seasons and/or three habitats were examined using permutation pairwise comparisons as *post hoc* tests on the season and site main effects. All data are presented as mean ± standard deviation unless otherwise stated. All data figures and fitting curves were generated using DataGraph 4.7.1 software (Visual Data Tools, Inc., Chapel Hill, North Carolina, USA). The extreme outliers were excluded from the statistical analysis and subsequent figures. To further study the ratio of net organic metabolism (net community production; NCP) and net inorganic metabolism [net community calcification; NCC; (Cyronak et al., 2018)], $nA_T$ values and $nC_T$ values at three sites in four seasons were plotted separately to create a least squares fitting curve using a linear regression model. The obtained slope was grouped with corresponding temperature and generated a least squares fitting curve using the linear regression model to study the relationship of the $nA_T$ - $nC_T$ slope and temperature. As the relative variation of $nA_T$ and $nC_T$ follows a well-established stoichiometry that is specific to the respective biogeochemical process, where the ratio for photosynthesis/respiration is –0.2 and the ratio for carbonate dissolution/calcification is 2.0 (Krumins et al., 2013; Sippo et al., 2016), the relative percent influence of NCP on changes in $nC_T$ was calculated according to the following formula (Cyronak et al., 2018):

$$\% \text{ NCP} = \frac{2 - slope}{2.2} \times 100\%$$

where the slope is the slope of $nA_T$ - $nC_T$ vector.

Since the correlation of $p$CO$_2$ and DO has been shown to have implications for upper ocean metabolic status, i.e., primary production/respiration and their history (Zhai et al., 2009), the $p$CO$_2$ and DO values were grouped together, creating a least squares fitting curve using the non-linear exponential regression model.

## RESULTS

### Seawater Carbonate Chemistry ($nA_T$, $nC_T$, and $n$pH$_T$)

The means with standard deviations and the variation ranges of seawater $nA_T$, $nC_T$, and $n$pH$_T$ at three macroalgal sits in four seasons are presented in **Table 1**, and the diel patterns of these three parameters are shown in **Figure 2**. In general, $nA_T$ ranged

**TABLE 1 |** The mean ± standard deviation (SD) and variation range of seawater carbonate parameters (salinity normalized total alkalinity: $nA_T$, salinity normalized total dissolved inorganic carbon: $nC_T$, and temperature normalized pH total scale: $npH_T$,) of three macroalgal habitats (UAM: ulvoid algal mat; TAM: turf algal mat; SC: coexisting *Sargassum horneri* and crustose coralline algae) in four seasons.

| Sites | Parameters | Winter | Spring | Summer | Autumn |
|---|---|---|---|---|---|
| | | Mean ± SD(Range) | Mean ± SD(Range) | Mean ± SD(Range) | Mean ± SD(Range) |
| UAM | $nA_T$ (µmol kg$^{-1}$) | 2219.7 ± 17.7 (2204.5 – 2251.6) | 2226.6 ± 16.4 (2203.4 – 2255.6) | 2234.6 ± 20.4 (2207.3 – 2258.6) | 2298.5 ± 8.9 (2289.9 – 2318.9) |
| | $nC_T$ (µmol kg$^{-1}$) | 1962.1 ± 34.9 (1906.9 – 2023.1) | 2021.5 ± 83.6 (1884.6 – 2137.3) | 2016.8 ± 19.0 (1995.7 – 2049.7) | 2087.9 ± 20.6 (2058.6 – 2117.2) |
| | $npH_T$ | 7.99 ± 0.08 (7.87 – 8.13) | 7.91 ± 0.15 (7.74 – 8.15) | 7.92 ± 0.08 (7.81 – 8.01) | 7.92 ± 0.05 (7.86 – 8.01) |
| TAM | $nA_T$ (µmol kg$^{-1}$) | 2205.9 ± 1.9 (2202.0 – 2209.4) | 2218.2 ± 4.6 (2208.7 – 2225.6) | 2220.7 ± 6.8 (2212.0 – 2231.9) | 2302.8 ± 13.6 (2287.2 – 2329.4) |
| | $nC_T$ (µmol kg$^{-1}$) | 1989.1 ± 14.2 (1964.3 – 2012.7) | 2001.8 ± 33.6 (1952.8 – 2055.2) | 1972.1 ± 24.7 (1931.8 – 2006.9) | 2095.9 ± 13.7 (2077.6 – 2118.7) |
| | $npH_T$ | 7.93 ± 0.04 (7.86 – 7.99) | 7.90 ± 0.07 (7.78 – 8.01) | 7.99 ± 0.06 (7.92 – 8.06) | 7.91 ± 0.04 (7.86 – 7.96) |
| SC | $nA_T$ (µmol kg$^{-1}$) | 2210.7 ± 3.1 (2203.9 – 2215.7) | 2232.8 ± 13.9 (2209.9 – 2251.3) | 2201.5 ± 7.1 (2189.0 – 2213.0) | 2295.5 ± 7.6 (2281.9 – 2304.0) |
| | $nC_T$ (µmol kg$^{-1}$) | 1953.7 ± 77.4 (1821.3 – 2045.3) | 2035.0 ± 100.4 (1887.5 – 2161.3) | 1957.4 ± 62.4 (1870.6 – 2030.0) | 2033.2 ± 102.9 (1793.7 – 2108.7) |
| | $npH_T$ | 7.99 ± 0.15 (7.80 – 8.23) | 7.87 ± 0.18 (7.63 – 8.12) | 7.98 ± 0.12 (7.83 – 8.17) | 7.99 ± 0.10 (7.89 – 8.16) |

from 2203.4 to 2318.9 µmol kg$^{-1}$ at the UAM site, and from 2202.0 to 2329.4 µmol kg$^{-1}$ at the TAM site, besides from 2189.0 to 2304.0 µmol kg$^{-1}$ at the SC site within four seasons. $nC_T$ values had a range from 1793.7 to 2161.3 µmol kg$^{-1}$ among all collected data. The highest value of $npH_T$ (8.23) was at the SC site in winter, and the lowest value (7.63) was at the SC site in spring. Salinity values were relatively stable in winter and spring (around 34 ‰), then decreased to approximately 32 ‰ in summer and autumn ( **Supplementary Table S3**). Overall, $nA_T$ values differed among seasons (PERMANOVA: Pseudo-$F_{3,199}$ = 566.280, $P_{(perm)}$ < 0.001) and the macroalgal habitat types (Pseudo-$F_{2,199}$ = 13.429, $P_{(perm)}$ < 0.001), and these two factors interacted with each other (Season × Site interaction: Pseudo-$F_{6,199}$ = 11.467, $P_{(perm)}$ < 0.001) (**Table 2**). However, this interaction explained very little (5%) of the total variation in $nA_T$ values. In contrast, differences among seasons explained most of the total variation in $nA_T$ (86%), with the mean values in winter (2212.1 ± 11.8 µmol kg$^{-1}$), spring (2225.9 ± 13.8 µmol kg$^{-1}$), summer (2219.0 ± 18.7 µmol kg$^{-1}$), and autumn (2299.2 ± 10.8 µmol kg$^{-1}$) all being significantly different from one another (permutation *post hoc* tests: $P \leq 0.015$ for each comparison). In contrast, differences among sites explained only 1% of the variation in $nA_T$, with the mean values at the UAM site (2241.2 ± 34.4 µmol kg$^{-1}$) being significantly higher than values at the TAM (2233.4 ± 38.5 µmol kg$^{-1}$) and the SC (2230.0 ± 35.0 µmol kg$^{-1}$) sites (permutation *post hoc* tests: $P$ < 0.001 for each comparison). $nA_T$ values did not differ between at the TAM and SC sites ($P$ = 0.193). $nC_T$ values also varied among seasons (PERMANOVA: Pseudo-$F_{3,203}$ = 33.837, $P_{(perm)}$ < 0.001) and sites with different macroalgal habitat types (Pseudo-$F_{2,203}$ = 4.276, $P_{(perm)}$ = 0.015), and these factors interacted with each other (Season × Site interaction: Pseudo-$F_{6,203}$ = 3.263, $P_{(perm)}$ = 0.007) (**Tables 1**, **2** and **Figure 2**). However, this interaction again explained very little (7%) of the total variation in $nC_T$. In contrast, differences among seasons explained far more of the variation in $nC_T$ (34%), with

mean values in winter (1968.5 ± 50.8 µmol kg$^{-1}$ SW), spring (2019.4 ± 77.4 µmol kg$^{-1}$), summer (1982.1 ± 47.0 µmol kg$^{-1}$), and autumn (2072.3 ± 66.1 µmol kg$^{-1}$) all being significantly different from one another (permutation *post hoc* tests: $P$ < 0.01 for each comparison), with an exception of the difference between winter and summer, which was not statistically different from one another ($P$ = 0.104). Differences among sites again explained very little (3%) of the variation in $nC_T$, with the values at the UAM site (2015.4 ± 64.7 µmol kg$^{-1}$) being significantly higher than those at the SC site (1990.8 ± 93.3 µmol kg$^{-1}$) (permutation *post hoc* test: $P$ = 0.013). Otherwise, $nC_T$ values did not differ between the TAM site (2011.9 ± 51.2 µmol kg$^{-1}$) and either the SC site ($P$ = 0.065) or the UAM site ($P$ = 0.232). Lastly, $npH_T$ values varied among seasons (PERMANOVA: Pseudo-$F_{3, 201}$ = 6.589, $P_{(perm)}$ = 0.002) but they did not vary among sites with different macroalgal habitat types (Pseudo-$F_{2,201}$ = 1.336, $P_{(perm)}$ = 0.265) (**Tables 1**, **2** and **Figure 2**). As with $nA_T$ and $nC_T$, these factors interacted with each other (Season × Site interaction: Pseudo-$F_{6,201}$ = 2.301, $P_{(perm)}$ = 0.033), but this interaction again explained very little (7%) of the variation in $npH_T$. Unlike with $nA_T$ and $nC_T$, however, differences among seasons only explained 9% of the total variation in $npH_T$, but values in spring (7.89 ± 0.14) were significantly lower than values in winter (7.97 ± 0.10), summer (7.96 ± 0.09), and autumn (7.94 ± 0.07) (permutation *post hoc* tests: $P$ = 0.001, 0.028, 0.003, respectively). Otherwise, $npH_T$ values did not vary among the other seasons ($P$ > 0.08 for each comparison).

The values of $nC_T$ and $npH_T$ covaried but in opposite directions in terms of diel variations, with $nC_T$ decreasing during the day and increasing at night, while $npH_T$ increased during the day and decreased at night (**Figure 2**). The largest $nC_T$ fluctuation occurred at the SC site in autumn (1793.7 to 2108.7 µmol kg$^{-1}$), and the largest $npH_T$ fluctuations occurred at the SC site in spring (7.63 to 8.12, **Table 1**). The smallest $nC_T$ and $npH_T$ fluctuation occurred at the TAM site in autumn (2077.6 to 2118.7
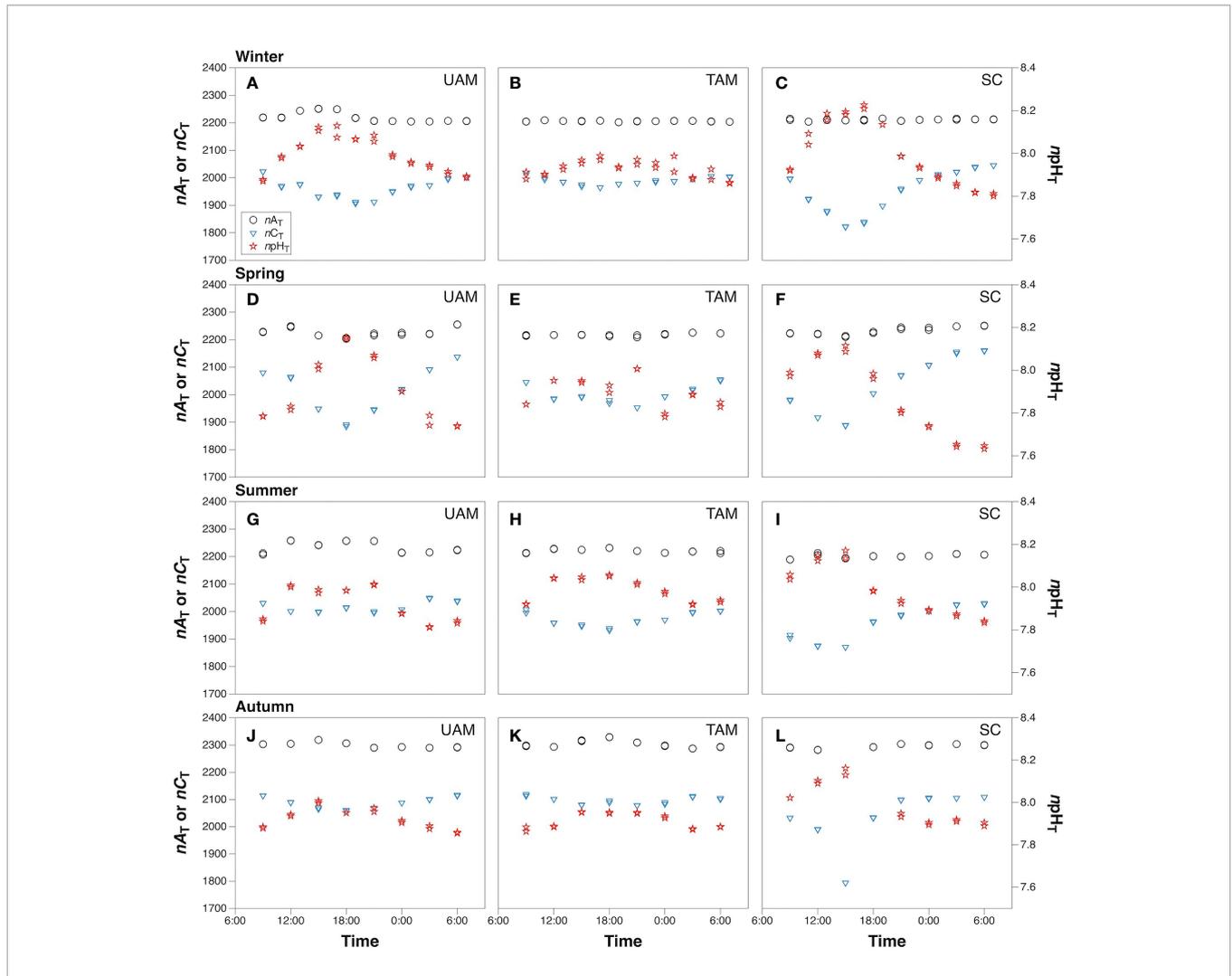
**FIGURE 2** | The diel variation of salinity normalized total alkalinity ($nA_T$, μmol kg$^{-1}$), salinity normalized total inorganic carbon ($nC_T$, μmol kg$^{-1}$) and temperature normalized pH total scale ($npH_T$) at three sites with different macroalgal habitats (UAM, ulvoid algal mat; TAM, turf algal mat; SC, coexisting *Sargassum horneri* and crustose coralline algae) in winter **(A–C)**, spring **(D–F)**, summer **(G–I)** and autumn **(J–L)**. Black circles represent values of $nA_T$, black triangles represent values of $nC_T$, and red stars represent values of $npH_T$.

**TABLE 2** | Results of two factor Model I PERMANOVAs testing the effects of season and site on seawater carbonate parameters (salinity normalized total alkalinity: $nA_T$, salinity normalized total dissolved inorganic carbon: $nC_T$, and temperature normalized pH total scale: $npH_T$).

| Parameters | Source | df | SS | MS | Psuedo-*F* | $P_{(perm)}$ | $\omega^2$ |
|---|---|---|---|---|---|---|---|
| $nA_T$ | Season | 3 | 25.708 | 8.5695 | 566.28 | 0.001 | 0.86 |
| | Site | 2 | 0.40643 | 0.20321 | 13.429 | 0.001 | 0.01 |
| | Season × Site | 6 | 1.0411 | 0.17352 | 11.467 | 0.001 | 0.05 |
| | Residual | 199 | 3.0115 | 1.51E-02 | | | 0.08 |
| $nC_T$ | Season | 3 | 42.874 | 14.291 | 33.837 | 0.001 | 0.34 |
| | Site | 2 | 3.6121 | 1.806 | 4.2761 | 0.015 | 0.03 |
| | Season × Site | 6 | 8.2687 | 1.3781 | 3.263 | 0.006 | 0.07 |
| | Residual | 203 | 85.738 | 0.42235 | | | 0.56 |
| $npH_T$ | Season | 3 | 6.46E-3 | 2.15E-3 | 6.5892 | 0.002 | 0.09 |
| | Site | 2 | 8.73E-4 | 4.37E-4 | 1.3364 | 0.265 | <0.01 |
| | Season × Site | 6 | 4.51E-3 | 7.52E-4 | 2.3014 | 0.033 | 0.06 |
| | Residual | 201 | 6.57E-2 | 3.27E-4 | | | 0.84 |

*The magnitudes of effect ($\omega^2$) represent the percentage of variation in each response variable that is explained by each factor in the models.*

$\mu$mol kg$^{-1}$, 7.86 to 7.96 respectively). $nA_T$ showed similar patterns with $nC_T$ at the SC site, though the range of $nA_T$ variations was smaller than that of $nC_T$. In contrast, $nA_T$ had opposite patterns to $nC_T$ at the UAM and TAM sites except in spring.

The relationships of $nA_T$ and $nC_T$ at three sites in four seasons are shown in **Figure 3**. The winter $nA_T/nC_T$ slopes for all three habitats were generally low (UAM: −0.124, TAM: −0.021, and SC: 0.017), leading to the high relative percent influence of NCP on changes in $nC_T$ from 90.14% to 96.56% (**Table 3**). The spring $nA_T/nC_T$ slopes increased slightly compared to winter slopes (UAM: 0.156, TAM: 0.077, and SC: 0.134), with an averaged % NCP value of 85.33 ± 1.85%. The $nA_T/nC_T$ slopes in summer and autumn showed values lower than −0.2% (i.e., summer: −0.724 at UAM site and −0.219 at TAM site; autumn: −0.593 at TAM site),

which led to the % NCP values over than 100%. The linear regression models (**Figure 4**) showed that the relationships of $nA_T/nC_T$ slopes with temperature were negative at the UAM and TAM sites (slopes: −0.051 at the UAM site and −0.035 at the TAM site), whereas slightly positive at the SC site (slope: 0.002). However, none of these three regressions were statistically significant.

## *In-Situ* Monitoring Seawater Biogeochemical Parameters ($p$CO$_2$, DO, and pH$_{NIST}$)

*In-situ* monitoring of biogeochemical parameters ($p$CO$_2$, DO, and pH$_{NIST}$) at the three sites characterized by different macroalgal types and four seasons are presented in **Table 4**, and their diel patterns are shown in **Figure 5**. Generally, $p$CO$_2$
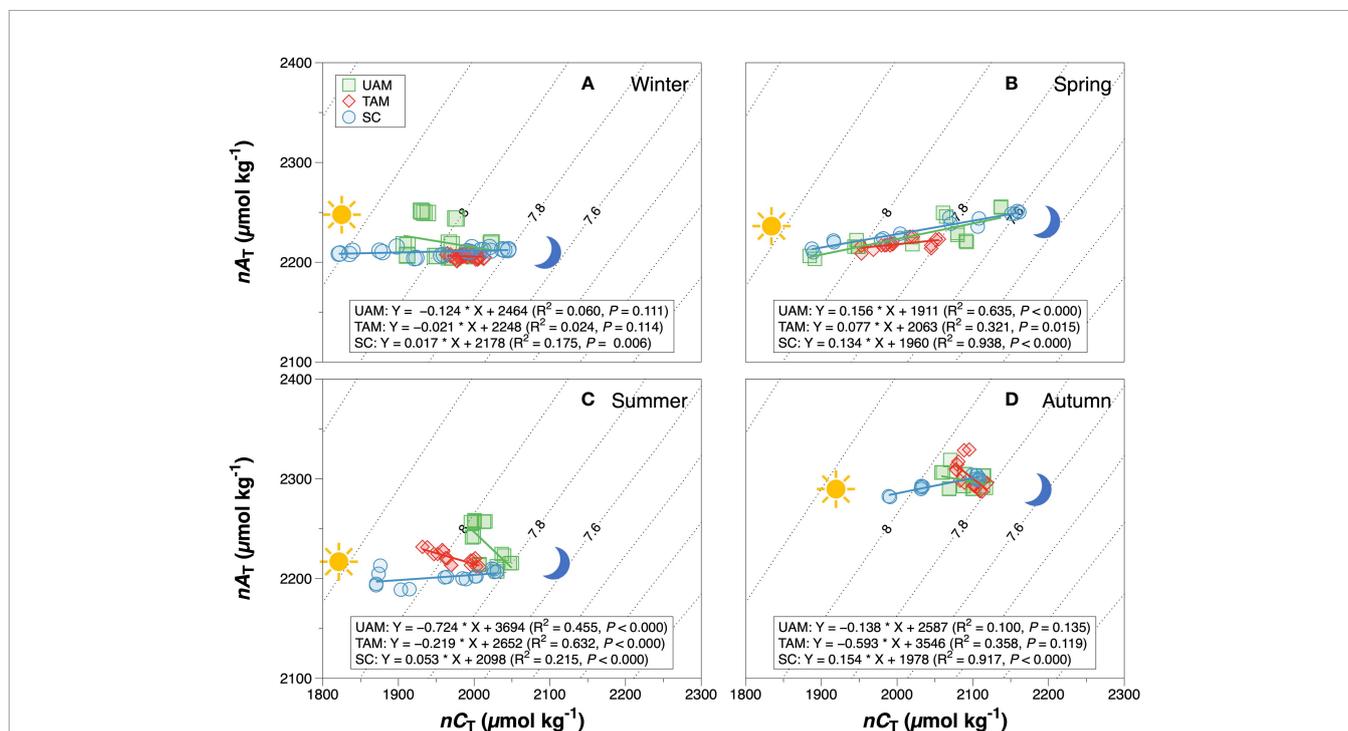


**FIGURE 3** | The relationship between salinity normalized total alkalinity ($nA_T$) and salinity normalized total inorganic carbon ($nC_T$) at three macroalgal habitats with different macroalgal habitats in winter **(A)**, spring **(B)**, summer **(C)** and autumn **(D)**. The solid lines are the least square fitting curve of data using the linear regression model. The dashed lines are pH isolines at 0.2 units increments with the 7.6 – 8.0 pH isoline indicated. pH contours were calculated using the averaged seawater temperature and salinity in each season. Values for different macroalgal habitats: ulvoid algal mat (UAM, green square); turf algal mat (TAM, red diamond); coexisting *Sargassum horneri* and crustose coralline algae (SC, blue circle).

**TABLE 3** | The slope of the salinity normalized total alkalinity ($nA_T$) – salinity normalized total inorganic carbon ($nC_T$) vector and the relative percent influence of net community production (%NCP) on changes in $nC_T$ at three habitat sites (UAM, ulvoid algal mat; TAM, turf algal mat; SC, coexisting *Sargassum horneri* and crustose coralline algae) in four seasons.

| Season | UAM | | TAM | | SC | |
|---|---|---|---|---|---|---|
| | Slope | % NCP | Slope | % NCP | Slope | % NCP |
| Winter | −0.124 | 96.56 | −0.021 | 91.86 | 0.017 | 90.14 |
| Spring | 0.156 | 83.80 | 0.077 | 87.39 | 0.134 | 84.80 |
| Summer | −0.724 | 123.80 | −0.219 | 100.85 | 0.053 | 88.51 |
| Autumn | −0.138 | 97.18 | −0.593 | 117.87 | 0.154 | 83.92 |
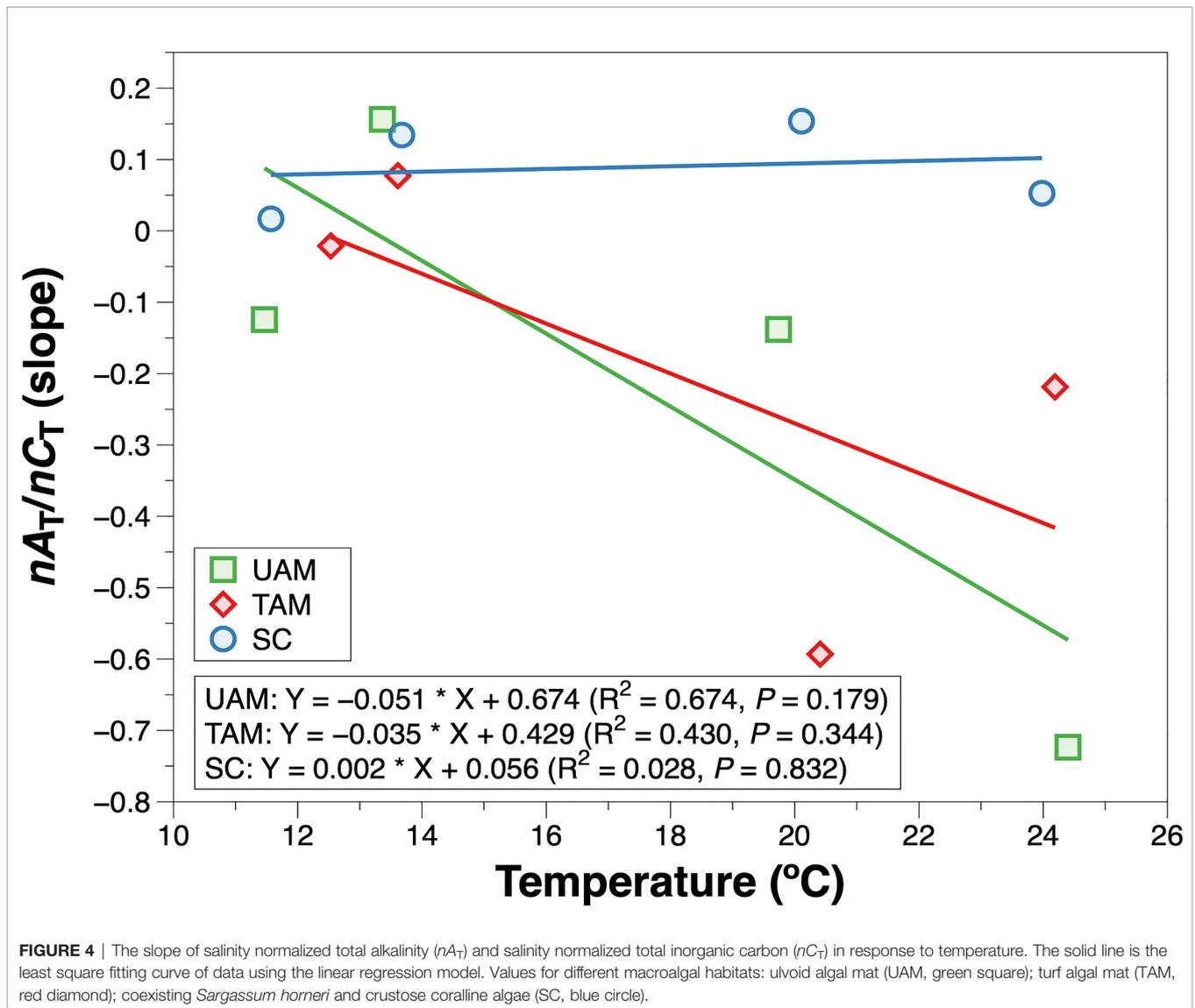
**FIGURE 4** | The slope of salinity normalized total alkalinity ($nA_T$) and salinity normalized total inorganic carbon ($nC_T$) in response to temperature. The solid line is the least square fitting curve of data using the linear regression model. Values for different macroalgal habitats: ulvoid algal mat (UAM, green square); turf algal mat (TAM, red diamond); coexisting *Sargassum horneri* and crustose coralline algae (SC, blue circle).

values, paralleled temperature values (**Supplementary Table S3**), being lowest in winter, increasing in spring, and then remaining high in summer and autumn at all three macroalgal sites. In contrast, DO and $pH_{NIST}$ values had relatively high values in winter and spring, then decreased in summer and autumn. Further statistical analysis showed that $pCO_2$ values varied among seasons (PERMANOVA: Pseudo-$F_{3,978}$ = 586.43, $P_{(perm)}$ < 0.001) and sites with different macroalgal habitat types (Pseudo-$F_{2,978}$ = 59.93, $P_{(perm)}$ < 0.001), and these two factors interacted with each other (Season × Site interaction: Pseudo-$F_{6,978}$ = 77.40, $P_{(perm)}$ < 0.001) (**Table 5**). However, differences among seasons explained the largest amount of variation in $pCO_2$ values (54%), while differences among sites explained only 4% of this variation and the interaction between season and site explained 21% of this variation. Overall, $pCO_2$ values were highest in autumn (522.33 ± 91.79 µatm), followed by summer (465.13 ± 95.01 µatm), then by spring (398.78 ±

152.47 µatm), and then by winter (256.64 ± 71.36 µatm), all of which were significantly different from each other (permutation *post hoc* tests: $P$ < 0.01 for each comparison). The mean $pCO_2$ value at the TAM site (394.82 ± 110.50 µatm) was significantly higher than the mean values at both the UAM site (376.01 ± 214.89 µatm) and the SC site (339.92 ± 85.18 µatm), all of which were significantly different from each other ($P$ < 0.01 for each comparison). Similarly, DO values also varied among seasons (PERMANOVA: Pseudo-$F_{3,6106}$ = 2614.3, $P_{(perm)}$ < 0.001) and sites with different macroalgal habitat types (Pseudo-$F_{2,6106}$ = 185.64, $P_{(perm)}$ < 0.001), and these two factors interacted with each other (Season × Site interaction: Pseudo-$F_{6,6106}$ = 226.31, $P_{(perm)}$ < 0.001) (**Table 5**). As with $pCO_2$, differences among seasons explained the larges amount of the total variations in DO (54%), while differences among sites explained only 3% and the interaction between season and site explained 14% of this variation. Overall, mean DO values were greatest in winter

**TABLE 4 |** The mean ± standard deviation (SD) and variation range of the *in-situ* monitoring parameters (partial pressure of $CO_2$: $pCO_2$, dissolved oxygen: DO, and pH on the scale of National Institute of Standards and Technology: $pH_{NIST}$) of three macroalgal habitats (UAM: ulvoid algal mat; TAM: turf algal mat; SC: coexisting *Sargassum horneri* and crustose coralline algae) in four seasons.

| Sites | Parameters | Winter | Spring | Summer | Autumn |
|---|---|---|---|---|---|
| | | Mean ± SD(Range) | Mean ± SD(Range) | Mean ± SD(Range) | Mean ± SD(Range) |
| UAM | $pCO_2$ (µatm) | 204.68 ± 94.74 (84.36 − 528.94) | 423.58 ± 201.92 (165.15 − 997.17) | 564.24 ± 156.75 (256.66 − 829.29) | 613.61 ± 62.44 (488.75 − 724.06) |
| | DO (mg L$^{-1}$) | 13.32 ± 3.63 (5.72 − 20.93) | 11.44 ± 3.37 (4.71 − 18.52) | 6.47 ± 2.00 (3.61 − 12.37) | 7.03 ± 0.37 (6.38 − 7.79) |
| | $pH_{NIST}$ | 8.50 ± 0.17 (8.11 − 8.81) | 8.21 ± 0.17 (7.77 − 8.53) | 8.08 ± 0.11 (7.90 − 8.37) | 7.99 ± 0.05 (7.91 − 8.09) |
| TAM | $pCO_2$ (µatm) | 284.21 ± 39.68 (172.59 − 363.38) | 483.31 ± 89.11 (318.30 − 683.18) | 431.82 ± 51.18 (318.00 − 545.32) | 508.41 ± 36.74 (459.40 − 576.38) |
| | DO (mg L$^{-1}$) | 10.51 ± 0.87 (8.82 −12.77) | 9.32 ± 1.19 (7.27 − 11.96) | 7.64 ± 1.15 (6.08 − 11.34) | 7.81 ± 0.57 (6.68 − 8.68) |
| | $pH_{NIST}$ | 8.35 ± 0.05 (8.25 − 8.46) | 8.12 ± 0.10 (7.93 − 8.31) | 8.16 ± 0.05 (8.00 − 8.30) | 8.06 ± 0.03 (8.00 − 8.12) |
| SC | $pCO_2$ (µatm) | 281.04 ± 26.67 (225.84 − 340.77) | 289.46 ± 41.59 (230.01 − 373.49) | 455.00 ± 58.31 (361.60 − 557.91) | 413.71 ± 29.94 (280.42 − 450.73) |
| | DO (mg L$^{-1}$) | 11.26 ± 0.69 (9.73 − 13.19) | 12.21 ± 1.08 (9.91 − 14.52) | 7.53 ± 0.41 (6.72 − 8.50) | 8.53 ± 0.09 (8.34 − 8.86) |
| | $pH_{NIST}$ | 8.37 ± 0.03 (8.30 − 8.46) | 8.31 ± 0.06 (8.21 − 8.41) | 8.13 ± 0.05 (8.05 − 8.23) | 8.13 ± 0.02 (8.09 − 8.20) |
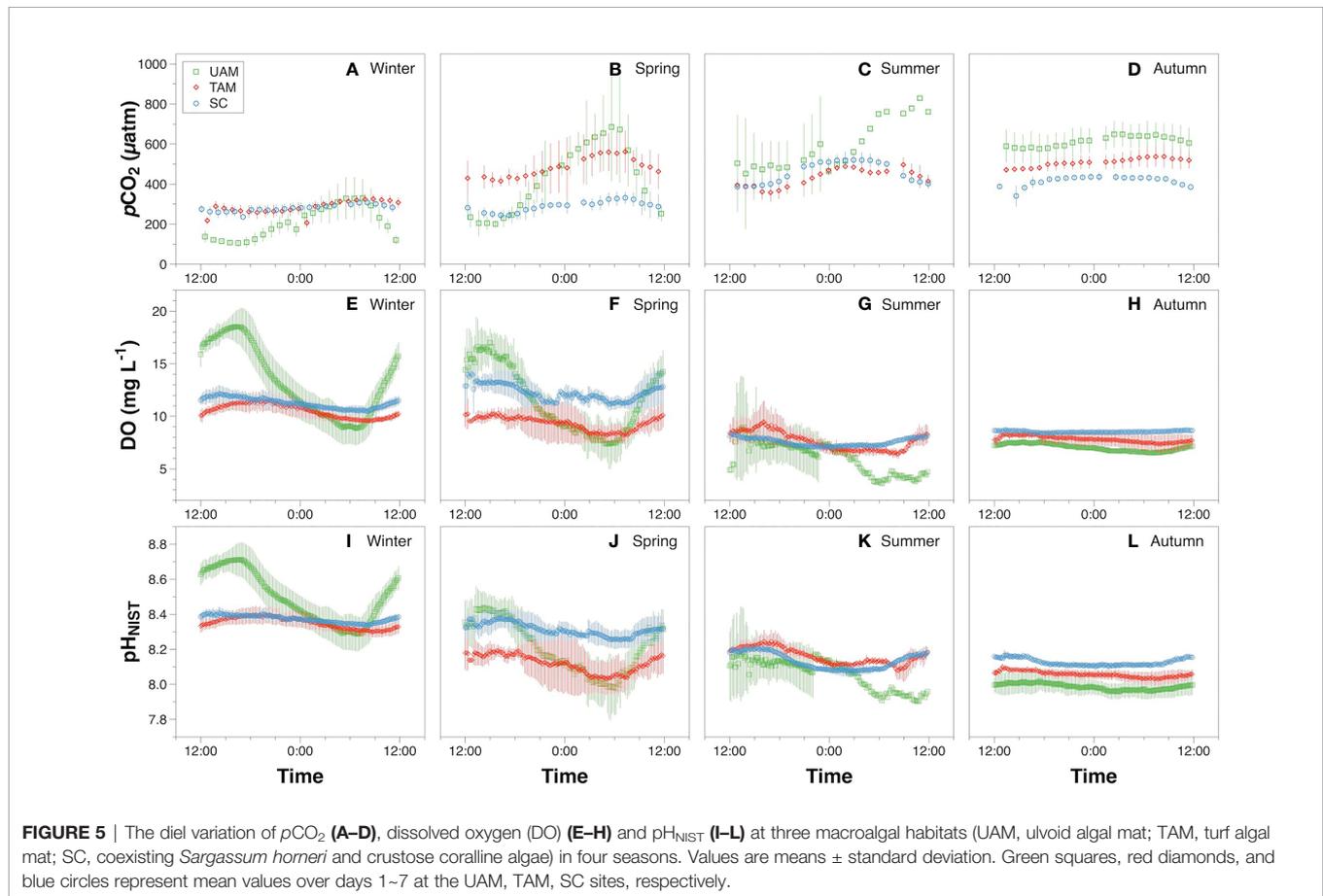


**FIGURE 5 |** The diel variation of $pCO_2$ **(A–D)**, dissolved oxygen (DO) **(E–H)** and $pH_{NIST}$ **(I–L)** at three macroalgal habitats (UAM, ulvoid algal mat; TAM, turf algal mat; SC, coexisting *Sargassum horneri* and crustose coralline algae) in four seasons. Values are means ± standard deviation. Green squares, red diamonds, and blue circles represent mean values over days 1~7 at the UAM, TAM, SC sites, respectively.

**TABLE 5 |** Results of two factor Model I PERMANOVAs testing the effects of season and site on the *in-situ* monitoring parameters (partial pressure of $CO_2$: $pCO_2$, dissolved oxygen concentration: DO, and pH on the scale of National Institute of Standards and Technology: $pH_{NIST}$). The magnitudes of effect ($\omega^2$) represent the percentage of variation in each response variable that is explained by each factor in the models.

| Parameters | Source | df | SS | MS | Psuedo-F | $P_{(perm)}$ | $\omega^2$ |
|---|---|---|---|---|---|---|---|
| $pCO_2$ | Season | 3 | 7805.2 | 2601.7 | 586.43 | 0.001 | 0.54 |
| | Site | 2 | 531.8 | 265.9 | 59.934 | 0.001 | 0.04 |
| | Season × Site | 6 | 2060.4 | 343.4 | 77.403 | 0.001 | 0.21 |
| | Residual | 978 | 4338.9 | 4.4365 | | | 0.21 |
| DO | Season | 3 | 557.96 | 185.99 | 2614.3 | 0.001 | 0.55 |
| | Site | 2 | 26.415 | 13.207 | 185.64 | 0.001 | 0.03 |
| | Season × Site | 6 | 96.601 | 16.1 | 226.31 | 0.001 | 0.14 |
| | Residual | 6106 | 434.4 | 7.1143E-2 | | | 0.29 |
| $pH_{NIST}$ | Season | 3 | 3.6713 | 1.2238 | 4890.40 | 0.001 | 0.64 |
| | Site | 2 | 0.12341 | 6.17E-2 | 246.58 | 0.001 | 0.03 |
| | Season × Site | 6 | 0.56948 | 9.49E-2 | 379.29 | 0.001 | 0.15 |
| | Residual | 6043 | 1.5122 | 2.50E-4 | | | 0.18 |

$(11.70 \pm 2.49 \, mg \, L^{-1})$, followed by spring $(10.99 \pm 2.48 \, mg \, L^{-1})$, autumn $(7.71 \pm 0.72 \, mg \, L^{-1})$, and then summer $(7.37 \pm 1.25 \, mg \, L^{-1})$, all of which were significantly different from each other (permutation *post hoc* tests: $P < 0.01$ for each comparison). Further, the mean DO value was greatest at the SC site $(10.26 \pm 1.94 \, mg \, L^{-1})$, followed by UAM site $(10.77 \pm 4.12 \, mg \, L^{-1})$, and then the TAM site $(9.16 \pm 1.57 \, mg \, L^{-1})$, all of which were significantly different from each other $(P < 0.01$ for each comparison). As with DO and $pCO_2$, $pH_{NIST}$ varied among seasons (PERMANOVA: Pseudo-$F_{3,6043} = 4890.40$, $P_{(perm)} < 0.001$) and sites with different macroalgal habitat types (Pseudo-$F_{2,6043} = 246.58$, $P_{(perm)} < 0.001$), and these two factors interacted with each other (Season × Site interaction: Pseudo-$F_{6,6043} = 379.29$, $P_{(perm)} < 0.001$) (**Table 5**). Also, as with DO and $pCO_2$, differences among seasons explained the largest amount of variation in $pH_{NIST}$ (64%), while differences among sites explained only 3% of this variation and the interaction between season and site explained only 15% of this variation. Overall, $pH_{NIST}$ was highest in winter $(8.41 \pm 0.12)$, then decreased in spring $(8.21 \pm 0.14)$ and summer $(8.13 \pm 0.07)$, and reached their lowest values in autumn $(8.05 \pm 0.07)$, all of which were significantly different from each other (permutation *post hoc* tests: $P < 0.01$ for each comparison). Furthermore, although $pH_{NIST}$ values appeared very similar, $pH_{NIST}$ at the SC site $(8.27 \pm 0.12)$, the UAM site $(8.27 \pm 0.26)$, and the TAM site $(8.21 \pm 0.14)$ were each significantly different from one another $(P < 0.05$ for each comparison).

The diel variation of DO, $pCO_2$ and $pH_{NIST}$ within the three habitat sites and four seasons all varied significantly among seasons and habitats (**Tables 4**, **5** and **Figure 5**). Generally, DO and $pH_{NIST}$ exhibited similar patterns of diel fluctuations (i.e., increasing during the day and decreasing during the night), which were opposite to the fluctuation patterns in $pCO_2$. The UAM site in summer had abnormal patterns of these three parameters since a typhoon occurred during the monitoring period. DO in winter at the UAM site had the largest fluctuation, from 5.72 to 20.93 $mg \, L^{-1}$ and with an average value of $13.32 \pm 3.63 \, mg \, L^{-1}$. In contrast, DO in autumn at the SC site had the smallest fluctuation, from 8.34 to 8.86 $mg \, L^{-1}$. Both lowest and highest $pH_{NIST}$ values occurred at the UAM site in spring (7.77) and winter (8.81). The largest and smallest fluctuation of $pCO_2$ was at the UAM site in spring (165.15 to 997.17 μatm) and at the SC site in winter (225.84 to 340.77 μatm). Furthermore, $pCO_2$

and DO values in all groups had significantly negative exponential correlations (**Figure 6**). The UAM site had higher regression coefficients ($r^2$) over 0.9 among four seasons except in autumn ($r^2 = 0.33$). The TAM site had $r^2$ over 0.9 in spring and autumn. The SC site generally had a small range of DO and $pCO_2$, as well as low $r^2$ compared to UAM and TAM sites.

## DISCUSSION

We utilized two experimental approaches to investigate diel and seasonal variations in seawater chemistry in order to evaluate how macroalgal community metabolism or/and habitat characters *per se* influence the seawater chemistry signatures. First, the normalized carbonate chemistry parameters (i.e., $nA_T$, $nC_T$ and $npH_T$) were used to compare the effects of biological metabolism after the influences of temperature and salinity were removed by normalization. Hence, we believe that these results could represent the heterogeneity mainly induced by the metabolism of different macroalgal communities, even though they might not show the representative characters of each season. On the other hand, the DO, $pCO_2$, and $pH_{NIST}$ results were used to evaluate the combined effects of both environmental parameters and biological activities on biogeochemical features, which are more appropriate for the ecological implications. Unlike direct carbonate chemistry analysis, simultaneous *in-situ* monitoring between habitats was not possible because of the limitation in the number of sensors, but this limitation could be compensated by monitoring a wide range of fluctuations for several days. The limitations of above two approaches are complementary and their combined results are sufficient to explain the diel and seasonal heterogeneity among different types of macroalgal habitats.

## Diel and Seasonal Variations in Seawater Chemistry

The significant diel variations in seawater chemistry observed in our study were broadly consistent with previous investigations in macrophyte habitats (Chou et al., 2018; Murie and Bourdeau, 2020). Values of pH and DO shared similar diel patterns (i.e., increasing during the daytime and decreasing at nighttime), which

**FIGURE 6** | The relationship between $pCO_2$ and dissolved oxygen (DO) of three macroalgal habitats in winter **(A)**, spring **(B)**, summer **(C)** and autumn **(D)**. Solid lines are the least square fitting curves of data using the non-linear exponential regression model. Values for different macroalgal habitats: ulvoid algal mat (UAM, green square); turf algal mat (TAM, red diamond); coexisting *Sargassum horneri* and crustose coralline algae (SC, blue circle).

were opposite to the diel patterns of $nC_T$ and $pCO_2$. Such diel variation followed the metabolic patterns expected for macroalgae, with photosynthesis absorbing and releasing $CO_2$ during the daytime and nighttime, respectively. Besides, macroalgae also serve as habitats for numerous organisms (e.g., meiofauna, macrofauna, and fish) (Christie et al., 2009) and support higher densities of microbes (Weigel and Pfister, 2019). Hence, when evaluating the diel fluctuations of seawater chemistry, it should be kept in mind the contribution of fauna and microbes to community respirations, as well as calcifying organisms to calcification. In our study, the benthic macroflora accounted for over 85% of the total biomass of macroflora and macrofauna (**Supplementary Tables 1, 2**) at the TAM and SC sites. Moreover, each site has distinguished typical macroalgal communities as described in the study area of methods. Hence, even though macroalgae are not the sole drivers of seawater chemistry variation, it is meaningful to compare the heterogeneity of seawater chemistry from the view of different macroalgal communities. When only the biological metabolic effects of macroalgae were considered, the range of fluctuations in $nC_T$ and $npH_T$ was the most extensive at the SC site. Wide fluctuations in $nC_T$ and $npH_T$ at the SC site suggest that high rates of photosynthesis and calcification by CCA, and high productivity of canopy forming algae significantly affect carbonate chemistry parameters. However, the strong biological metabolism at the SC site was offset by hydrological characteristics. Specifically, when hydrological properties were considered, the ranges of DO, $pCO_2$, $pH_{NIST}$ at the UAM site were higher than

the ranges at the TAM and SC sites. This discrepancy suggests that diel fluctuations in carbonate chemistry may be affected by interactions between biological metabolism and environmental parameters. At first, ulvoid algae are opportunistic algae due to their high rates of nutrient uptake and then growth (Cohen and Fong, 2006; Bews et al., 2021), which could lead to a high amount of $CO_2$ influx *via* high rates of photosynthesis and respiration. Previous studies have shown that *Ulva* spp. had higher values of chlorophyll contents and the maximal quantum yield of photosystem II ($F_v/F_m$), an indicator of photosynthetic potential, than values of brown algae (e.g., *Sargassum* spp.) and red algae (e.g., *Grateloupia livida*) (Shi et al., 2021; Zhao et al., 2021). Carvalho and Eyre (2011) found that *Ulva* sp. had higher respiration rates than both brown and red algae (i.e., *Sargassum* sp. and *Pterocladia capillacea* Bornet). They believed it was because the thinner thallus enables *Ulva* to have more active cells per unit of carbon, as thinner primary producers have been observed to have higher respiration rates (Enríquez et al., 1996; Sand-Jensen and Nielsen, 2004). In addition, the UAM site is located in the inner harbor where there are direct sewage inputs. Hence, the relatively high nutrient concentrations might contribute to the high rates of metabolic activity (photosynthesis and respiration) in ulvoid algae, resulting in the largest fluctuation of DO and $pCO_2$ at UAM site (Bews et al., 2021). Furthermore, higher nutrient concentrations increased the biomass of microbes (Lebaron et al., 2001), and DO is consumed and $pCO_2$ is released due to microbial respiration as part of the overall degradation process of organic matter in the blooming area

(Chen et al., 2020). Therefore, biogeochemical fluctuations are more dynamically driven by photosynthesis of autotrophs, and respiration of autotrophs and microbial community. Another factor is that the seawater exchange with the open ocean is less at the UAM and TAM sites than at the SC site. The low rate of water exchange better highlighted the metabolic-induced variations (Semesi et al., 2009). In addition, the mixing between seawater and sewage containing high organic carbon also affected the carbonate chemistry of seawater (Kim et al., 2006). This might cause the abnormal ratios of $nA_T$ and $nC_T$ at the UAM and TAM sites in summer and autumn, which differed from the ratios at the SC site (**Figure 3**). Consequently, the heterogeneity of seawater chemistry across the three macroalgal habitats can be affected by both biological metabolisms and hydrological characteristics within the site.

The seasonal variation in seawater carbonate parameters among macroalgae habitats were also observed in other studies, though their patterns differed from those found in our study (Delille et al., 2000; Delille et al., 2009). Specifically, $pCO_2$ values in our study were lowest in winter and then increased in spring and summer, meanwhile DO values followed the opposite patterns. In contrast, Delille et al. (2009) found that $pCO_2$ values around kelp beds in the sub-Antarctic coast were relatively low in summer and spring, reached a high oversaturation of $pCO_2$ in autumn, and then decreased thereafter. These seasonal changes in the study of Delille et al. (2009) could be induced by the higher photosynthetic rates in spring and summer, and the decomposition of organic matter in autumn. A possible explanation for the difference of $pCO_2$ patterns between our study and Delille et al. (2009) might be the different ranges in seawater temperatures over seasons, and different growth patterns of the dominant macroalgae. In our study area, the variation of seawater temperature throughout the year was from 7.75 to 26.63°C, which was higher than the range (about 2 to 8°C) of sub-Antarctic coast in the study of Delille et al. (2009). In our study, the high temperature in summer (UAM: 23.03 to 24.93°C, TAM: 17.50 to 24.71°C, SC: 24.16 to 26.63°C) might inhibit the photosynthesis of macroalgae. For example, *Ulva* spp. has its highest growth rates at 15-20°C, and decreases in temperatures over 20°C (Taylor et al., 2001). Additionally, *Ulva australis* biomass along the south coast of Korean peaks in May and drops significantly in June, meanwhile photosynthetic rates are highest from January to March during the growth period and lowest from May to July when the biomass peaks or declines (Kim et al., 2004). Thus, our results indicate that the growth optimal temperature can be one of the potent factors for influencing the seawater biogeochemical parameters. However, it should be noted that our study focused on the investigation of seawater carbonate parameters without the measurements of biomass and photosynthetic performances of the corresponding macroalgae. Our data identified seasonal variation in seawater chemistry within macroalgal communities, but further studies could test the physiological performance of seaweed in different seasons to help understand how activities of seaweed affect the seawater carbon dynamics (Spector and Edwards, 2020). Furthermore, apart from the growth rhythms of macroalgae themselves, the abiotic factors also had important impacts on the metabolism of macroalgae.

Hence, besides temperature and salinity, water depth, light intensity, and nutrient concentration, the physical condition of seawater should be recorded in the further study to fully understand the process of seaweed communities altering the seawater carbonate conditions in a varying environment.

## Relationship of $nA_T$-$nC_T$

The relationship between $A_T$ and $C_T$ has been used as a tool to quantify the relative contributions of ecosystem metabolism to seawater chemistry changes occurring in various aquatic habitats (Dutta et al., 2019; Baldry et al., 2020; Saderne et al., 2020). The variation in stoichiometry between these two carbonate parameters represents relative intensities of biological activities including photosynthesis (and respiration), calcification (and dissolution), nitrification (and denitrification), sulfate reduction, and fermentation (Saderne et al., 2020). In our study, the slope values (relationships) in winter were from –0.12 to 0.02, indicating that photosynthesis and respiration were governing factors for carbon chemistry variations. Especially, the UAM and TAM sites had high % NCP values exceeding 90%. In spring, even though the slopes increased slightly compared to winter slopes, the activity of photosynthesis and respiration still were the major drivers of the carbonate chemistry dynamics. However, the slope values in summer and autumn were lower than –0.2, which appeared to violate the stoichiometry $nA_T/nC_T$ ratios predicted for photosynthesis/respiration. The abnormal phenomenon might be caused by the inflow of external water with different values of $nA_T$ in summer and autumn. As the UAM and TAM sites are located in the harbor, their seawater conditions are easy to be changed by the inflow of wastewater, especially in summer. The field investigation (Kim et al., 2004), in which the photosynthetic rate of ulvoid green algae was lowest in July, suggested that the low $nA_T/nC_T$ slopes in summer found in our study were not mainly caused by the photosynthesis of macroalgae. Actually, previous studies have shown that the magnitude of change along this $A_T$-$C_T$ ratio is driven by metabolic rates that are strongly dependent on physical factors including light intensity (Gattuso et al., 1996; Takeshita et al., 2016), residence time, and water depth (Falter et al., 2013). Our study further strengthened such viewpoint and highlighted that the wastewater might affect the seawater carbon dynamics within the short time scale.

## Relationship of $pCO_2$-DO

The relationship of $pCO_2$-DO depends on several physical (e.g., temperature, salinity and air-sea exchange) and biological (e.g., photosynthesis, respiration, and calcification) processes (DeGrandpre et al., 1998). Studies have evaluated the ocean metabolic status *via* the analysis of combined $CO_2$ and $O_2$ data (DeGrandpre et al., 1997; DeGrandpre et al., 1998; Zhai et al., 2009). In our study, $pCO_2$ and DO values were negatively correlated (**Figure 5**), especially in winter and spring, which are consistent with previous findings (Noriega and Araujo, 2014). The oversaturation of DO corresponding to the low $pCO_2$ values in winter and spring, indicated that macroalgae possessed high photosynthesis rates during this period, which agrees with our $nA_T$-$nC_T$ data and the growth patterns of macroalgae in the Korean

coast (Kim et al., 2004). In addition, the UAM site had high $pCO_2$ values with unsaturated DO, suggesting that the aerobic respiration rates were high. Such condition might occur because the UAM site in the inner harbor was directly influenced by sewage inputs. Meanwhile, the rates of organic matter decomposition increased with rising temperature, leading to the low DO and high $pCO_2$ values in summer. Previous studies have shown that the nutrient and organic matter inputs from riverine outflows and sewage effluents have increased the occurrences of hypoxia and high $CO_2$ concentrations in many coastal waters (Borges et al., 2006; Diaz and Rosenberg, 2008). In autumn, the narrow ranges of $pCO_2$ and DO might be related to the decrease in macroalgae biomass after several storms. Even though the accurate investigation is lacking, we observed the obvious decline of macroalgae during the set-up of sensors in autumn. Altogether, results of $pCO_2$ and DO are important for understanding the variation in biological processes among different types of macroalgal habitats, and they could be used as an important biochemical indicator to understand the fate of carbon dioxide within macroalgal communities (e.g., possibly convert DO-based NCP to $CO_2$ based NCP).

### Ecological Implication

The average value of atmospheric $CO_2$ has risen to 415.48 ppm June 2021 due to anthropogenic activities (Dlugokencky and Tans, 2021), and is predicted to reach 936 ppm for the representative concentration pathway (RCP) 8.5 by 2100 (IPCC, 2013). As 20-30% of global emissions of $CO_2$ are absorbed by the ocean, seawater pH has decreased to 8.1 (Caldeira and Wickett, 2003) and will drop by 0.036 to 0.291 units for the RCPs 2.6-8.5 by 2081-2100 (IPCC, 2019). According to our $pCO_2$ and $pH_{NIST}$ data, averaged values of $pCO_2$ in winter and spring were lower than the current concentrations and $pH_{NIST}$ were higher than 8.1, which means seaweed communities could mitigate OA stress during their growth seasons when photosynthesis rates are high. In summer and autumn, however, seaweed communities might exacerbate the effects of OA through respiration, as average values of $pCO_2$ were higher than current average values. Specifically, the average $pCO_2$ increased to 522.33 ± 91.79 μatm in autumn, resulting the low $pH_{NIST}$ value of 8.05 ± 0.07. Again, such situations should consider both the condition of the macroalgae and ambient environmental factors, because as temperature increase, macroalgae began to die and decompose, resulting in decreased photosynthesis and increased aerobic respiration. Our investigation highlights that macroalgae serve dual roles in OA mitigation by decreasing OA stress during the winter and spring (the growing season), but worsening OA in summer and autumn.

## CONCLUSION

This study investigated the dynamics of carbonate chemistry and dissolved oxygen in the benthic macroalgal habitats, which in turn reflected how the metabolic activities of macroalgae regulated seawater chemistry and its implications for mitigating OA stress. Our results illustrated that macroalgal photosynthesis could largely mitigate the OA stress in winter and spring when photosynthesis is high. Meanwhile the high photosynthesis rates by the dominant

macroalgae also result in large diel fluctuations in seawater carbonate parameters in winter and spring. However, these mitigation effects were dependent on temperature, which determined the growth condition and photosynthetic rates of the macroalgae. Once temperature exceeds the optimum ranges for these macroalgae in summer and autumn, respiration rates can surpass photosynthesis rates, and macroalgal communities could reversely increase $CO_2$ concentrations, thereby enhancing OA stress. Our study highlights that the role of seaweeds in regulating the seawater chemistry, especially acidification, should be evaluated in a long-term scale considering their metabolic interactions with multi-environmental factors.

## DATA AVAILABILITY STATEMENT

The raw data supporting the conclusions of this article will be made available by the authors, without undue reservation.

## AUTHOR CONTRIBUTIONS

## FUNDING

## ACKNOWLEDGMENTS

## SUPPLEMENTARY MATERIAL

The Supplementary Material for this article can be found online at: https://www.frontiersin.org/articles/10.3389/fmars.2022.857153/full#supplementary-material

# REFERENCES

Anderson, M. J., and Walsh, D. C. (2013). PERMANOVA, ANOSIM, and the Mantel Test in the Face of Heterogeneous Dispersions: What Null Hypothesis are You Testing? *Ecol. Monogr.* 83, 557–574. doi: 10.1890/12-2010.1

Baldry, K., Saderne, V., McCorkle, D. C., Churchill, J. H., Agusti, S., and Duarte, C. M. (2020). Anomalies in the Carbonate System of Red Sea Coastal Habitats. *Biogeosciences* 17, 423–439. doi: 10.5194/bg-17-423-2020

Bews, E., Booher, L., Polizzi, T., Long, C., Kim, J.-H., and Edwards, M. S. (2021). Effects of Salinity and Nutrients on Metabolism and Growth of *Ulva lactuca*: Implications for Bioremediation of Coastal Watersheds. *Mar. Pollut. Bull.* 166, 112199. doi: 10.1016/j.marpolbul.2021.112199

Borges, A. V., Schiettecatte, L. S., Abril, G., Delille, B., and Gazeau, F. (2006). Carbon Dioxide in European Coastal Waters. *Estuar. Coast. Shelf. Sci.* 70, 375–387. doi: 10.1016/j.ecss.2006.05.046

Britton, D., Cornwall, C. E., Revill, A. T., Hurd, C. L., and Johnson, C. R. (2016). Ocean Acidification Reverses the Positive Effects of Seawater pH Fluctuations on Growth and Photosynthesis of the Habitat-Forming Kelp, *Ecklonia radiata*. *Sci. Rep.* 6, 26036. doi: 10.1038/srep26036

Cai, W. J., Xu, Y. Y., Feely, R. A., Wanninkhof, R., Jonsson, B., and Alin, S. R., et al (2020). Controls on Surface Water Carbonate Chemistry Along North American Ocean Margins. *Nat. Commun.* 11, 2691. doi: 10.1038/s41467-020-16530-z

Caldeira, K., and Wickett, M. E. (2003). Anthropogenic Carbon and Ocean pH. *Nature* 425, 365. doi: 10.1038/425365a

Carrano, M. W., Carrano, C. J., Edwards, M. S., Al-Adilah, H., Fontana, Y., Sayer, M. D. J., et al. (2021). *Laminaria* Kelps Impact Iodine Speciation Chemistry in Coastal Seawater. *Estuar. Coast. Shelf. Sci.* 262, 107531. doi: 10.1016/j.ecss.2021.107531

Carrano, M. W., Yarimizu, K., Conzales, J. L., Cruz-López, R., Edwards, M. S., Tymon, T., et al. (2020). The Influence of Marine Algae on Iodine Speciation in the Coastal Ocean. *Algae* 35, 167–176. doi: 10.4490/algae.2020.35.5.25

Carvalho, M. C., and Eyre, B. D. (2011). Carbon Stable Isotope Discrimination During Respiration in Three Seaweed Species. *Mar. Ecol. Prog. Ser.* 437, 41–49. doi: 10.3354/meps09300

Chen, J., Li, H., Zhang, Z., He, C., Shi, Q., Jiao, N., et al. (2020). DOC Dyanmics and Bacterial Community Succession During Long-Term Degradation of *Ulva prolifera* and Their Implications for the Legacy Effect of Green-Tides on Refractory DOC Pool in Seawater. *Water Res.* 185, 116268. doi: 10.1016/j.watres.2020.116268

Chou, W.-C., Chu, H.-C., Chen, Y.-H., Syu, R.-W., Hung, C.-C., and Soong, K. (2018). Short-Term Variability of Carbon Chemistry in Two Contrasting Seagrass Meadows at Dongsha Island: Implications for pH Buffering and $CO_2$ Sequestration. *Estuar. Coast. Shelf. Sci.* 210, 36–44. doi: 10.1016/j.ecss.2018.06.006

Christie, H., Norderhaug, K. M., and Fredriksen, S. (2009). Macrophytes as Habitat for Fauna. *Mar. Ecol. Prog. Ser.* 396, 221–233. doi: 10.3354/meps08351

Clayton, T. D., and Byrne, R. H. (1993). Spectrophotometric Seawater pH Measurements: Total Hydrogen Ion Concentration Scale Calibration of *M*-Cresol Purple and at-Sea Results. *Dee. Sea. Res. Part I. Oceanogr. Res. Pap.* 40, 2115–2129. doi: 10.1016/0967-0637(93)90048-8

Cohen, R. A., and Fong, P. (2006). Using Opportunistic Green Macroalgae as Indicators of Nitrogen Supply and Sources to Estuaries. *Ecol. Appl.* 16, 1405–1420. doi: 10.1890/1051-0761(2006)016[1405:UOGMAI]2.0.CO;2

Comeau, S., and Cornwall, C. E. (2016). "Contrasting Effects of Ocean Acidification on Coral Reef "Animal Forests" Versus Seaweed "Kelp Forests", in *Marine Animal Forests*. eds. S. Rossi, L. Bramanti, A. Gori and C. Orejas Saco del Valle (Cham: Springer), 1–25. doi: 10.1007/978-3-319-17001-5_29-1

Cyronak, T., Andersson, A. J., Langdon, C., Albright, R., Bates, N. R., Caldeira, K., et al. (2018). Taking the Metabolic Pulse of the World's Coral Reefs. *PloS One* 13, e0190872. doi: 10.1371/journal.pone.0190872

DeGrandpre, M. D., Hammar, T. R., Wallace, D. W. R., and Wirick, C. D. (1997). Simultaneous Mooring-Based Measurements of Seawater $CO_2$ and $O_2$ Off Cape Hatteras, North Carolina. *Limnol. Oceanogr.* 42, 21–28. doi: 10.4319/lo.1997.42.1.0021

DeGrandpre, M. D., Hammar, T. R., and Wirick, C. D. (1998). Short-Term $pCO_2$ and $O_2$ Dynamics in California Coastal Waters. *Deep. Sea. Res. Part II Top. Stud. Oceanogr.* 45, 1557–1575. doi: 10.1016/S0967-0645(98)80006-4

Delille, B., Borges, A. V., and Delille, D. (2009). Influence of Giant Kelp Beds (*Macrocystis pyrifera*) on Diel Cycles of $pCO_2$ and DIC in the Sub-Antarctic Coastal Area. *Estuar. Coast. Shelf. Sci.* 81, 114–122. doi: 10.1016/j.ecss.2008.10.004

Delille, B., Delille, D., Fiala, M., Prevost, C., and Frankignoulle, M. (2000). Seasonal Changes of $pCO_2$ Over a Subantarctic *Macrocystis* Kelp Bed. *Polar. Biol.* 23, 706–716. doi: 10.1007/s003000000142

Deng, X., Liu, T., Liu, C.-Y., Liang, S.-K., Hu, Y.-B., Jin, Y.-M., et al. (2018). Effects of *Ulva prolifera* Blooms on the Carbonate System in the Coastal Waters of Qingdao. *Mar. Ecol. Prog. Ser.* 605, 73–86. doi: 10.3354/meps12739

Diaz, R. J., and Rosenberg, R. (2008). Spreading Dead Zones and Consequences for Marine Ecosystems. *Science* 321, 926–929. doi: 10.1126/science.1156401

Dickson, A. G. (1993). The Measurement of Sea Water pH. *Mar. Chem.* 44, 131–142. doi: 10.1016/0304-4203(93)90198-W

Dickson A. G., Sabine C. L. and Christian J. R. (eds.) (2007). *Guide to Best Practices for Ocean CO2 Measurements* Vol. 3 (Sidney, BC: PICES Special Publication). doi: 10.25607/OBP-1342

Dlugokencky, E., and Tans, P. (2021) *Trends in Atmospheric Carbon Dioxide* (NOAA/GML). Available at: https://gml.noaa.gov/ccgg/trends/global.html (accessed Sep. 28, 2021).

Doney, S. C., Fabry, V. J., Feely, R. A., and Kleypas, J. A. (2009). Ocean Acidification: The Other $CO_2$ Problem. *Ann. Rev. Mar. Sci.* 1, 169–192. doi: 10.1146/annurev.marine.010908.163834

Dutta, M. K., Kumar, S., Mukherjee, R., Sharma, N., Acharya, A., Sanyal, P., et al. (2019). Diurnal Carbon Dynamics in a Mangrove-Dominated Tropical Estuary (Sundarbans, India). *Estuar. Coast. Shelf. Sci.* 229, 106426. doi: 10.1016/j.ecss.2019.106426

Edwards, M. S., Kornar, B., Kim, J.-H., Gabara, S., Sullaway, G., McHugh, T. A., et al. (2020). Marine Deforestation Leads to Widespread Loss of Ecosystem Function. *PloS One* 15, e0226173. doi: 10.1371/journal.pone.0226173

Enríquez, S., Duarte, C. M., Sand-Jensen, K., and Nielsen, S. L. (1996). Broad-Scale Comparison of Photosynthetic Rates Across Phototrophic Organisms. *Oecologia* 108, 197–206. doi: 10.1007/BF00334642

Falter, J. L., Lowe, R. J., Zhang, Z., and McCulloch, M. (2013). Physical and Biological Controls on the Carbonate Chemistry of Coral Reef Waters: Effects of Metabolism, Wave Forcing, Sea Level, and Geomorphology. *PloS One* 8, e53303. doi: 10.1371/journal.pone.0053303

Frieder, C. A., Nam, S. H., Martz, T. R., and Levin, L. A. (2012). High Temporal and Spatial Variability of Dissolved Oxygen and pH in a Nearshore California Kelp Forest. *Biogeosciences* 9, 3917–3930. doi: 10.5194/bg-9-3917-2012

Gattuso, J. P., Pichon, M., Delesalle, B., Canon, C., and Frankignoulle, M. (1996). Carbon Fluxes in Coral Reefs. I. Lagrangian Measurement of Community Metabolism and Resulting Air-Sea $CO_2$ Disequilibrium. *Mar. Ecol. Prog. Ser.* 145, 109–121. doi: 10.3354/meps145109

Gonzales, J., Tymon, T., Küpper, F. C., Edwards, M. S., and Carrano, C. J. (2017). The Potential Role of Kelp Forests on Iodine Speciation in Coastal Seawater. *PloS One* 12, e0180755. doi: 10.1371/journal.pone.0180755

Graham, M. H., and Edwards, M. S. (2001). Statistical Significance Versus Factor Fit: Estimating the Importance of Individual Factor in Ecological Analysis of Variance. *Oikos* 93, 505–513. doi: 10.1034/j.1600-0706.2001.930317.x

Hofmann, G. E., Smith, J. E., Johnson, K. S., Send, U., Levin, L. A., Micheli, F., et al. (2011). High-Frequency Dynamics of Ocean pH: A Multi-Ecosystem Comparison. *PloS One* 6, e28983. doi: 10.1371/journal.pone.0028983

IPCC (2013). Climate Change 2013: The Physical Science Basis. Contribution of Working Group I to the Fifth Assessment Report of the Intergovernmental Panel on Climate Change, eds. T. F. Stocker, D. Qin, G.-K. Plattner, M. Tignor, S. K. Allen, J. Boschung, et al. (Cambridge: Cambridge University Press), 1535. doi: 10.1017/CBO9781107415324

IPCC (2019). IPCC Special Report on the Ocean and Cryosphere in a Changing Climate. eds. H.-O. Pörtner, D. C. Roberts, V. Masson-Delmotte, P. Zhai, M. Tignor, E. Poloczanska, et al. Available at: https://www.ipcc.ch/report/srocc/ (accessed Oct. 25, 2021).

Kang, E. J., Han, A.-R., Kim, J.-H., Kim, I.-N., Lee, S., Min, J.-O., et al. (2021). Evaluating Bloom Potential of the Green-Tide Forming Alga *Ulva ohnoi* Under Ocean Acidification and Warming. *Sci. Total. Environ.* 769, 144443. doi: 10.1016/j.scitotenv.2020.144443

Kim, K. Y., Choi, T. S., Kim, J. H., Han, T., Shin, H. W., and Garbary, D. J. (2004). Physiological Ecology and Seasonality of *Ulva pertusa* on a Temperate Rocky Shore. *Phycologia* 43, 483–492. doi: 10.2216/i0031-8884-43-4-483.1

Kim, J.-H., Kang, E. J., Kim, K., Jeong, H. J., Lee, K., Edwards, M. S., et al. (2015). Evaluation of Carbon Fluxes in Vegetative Bay Based on Ecosystem Production and $CO_2$ Exchange Driven by Coastal Autotrophs. *Algae* 30, 121–137. doi: 10.4490/algae.2015.30.2.121

Kim, J.-H., Kim, N., Moon, H., Lee, S., Jeong, S. Y., Diaz-Pulido, G., et al. (2020a). Global Warming Offsets the Ecophysiological Stress of Ocean Acidification on Temperate Crustose Coralline Algae. *Mar. Pollut. Bull.* 157, 111324. doi: 10.1016/j.marpolbul.2020.111324

Kim, H.-C., Lee, K., and Choi, W. (2006). Contribution of Phytoplankton and Bacterial Cells to the Measured Alkalinity of Seawater. *Limnol. Oceanogr.* 51, 331–338. doi: 10.4319/lo.2006.51.1.0331

Kim, J.-M., Lee, K., Han, I.-S., Lee, J.-S., Choi, Y. H., Lee, J.-H., et al. (2020b). Anthropogenic Nitrogen-Induced Changes in Seasonal Carbonate Dynamics in a Productive Coastal Environment. *Geophys. Res. Lett.* 47, e2020GL088232. doi: 10.1029/2020GL088232

Ko, Y. H., Lee, K., Noh, J. H., Lee, C. M., Kleypas, J. A., Jeong, H. J., et al. (2016). Influence of Ambient Water Intrusion on Coral Reef Acidification in the Chuuk Lagoon, Located in the Coral-Rich Western Pacific Ocean. *Geophys. Ress. Lett.* 43, 3830–3838. doi: 10.1002/2016gl068234

Koweek, D. A., Nickols, K. J., Leary, P. R., Litvin, S. Y., Bell, T. W., Luthin, T., et al. (2017). A Year in the Life of a Central California Kelp Forest: Physical and Biological Insights Into Biogeochemical Variability. *Biogeosciences* 14, 31–44. doi: 10.5194/bg-14-31-2017

Krause-Jensen, D., Duarte, C. M., Hendriks, I. E., Meire, L., Blicher, M. E., Marbà, N., et al. (2015). Macroalgae Contribute to Nested Mosaics of pH Variability in a Subarctic Fjord. *Biogeosciences* 12, 4895–4911. doi: 10.5194/bg-12-4895-2015

Krumins, V., Gehlen, M., Arndt, S., Van Cappellen, P., and Regnier, P. (2013). Dissolved Inorganic Carbon and Alkalinity Fluxes From Coastal Marine Sediments: Model Estimates for Different Shelf Environments and Sensitivity to Global Change. *Biogeosciences* 10, 371–398. doi: 10.5194/bg-10-371-2013

Kuss, J., Roeder, W., Wlost, K. P., and DeGrandpre, M. D. (2006). Time-Series of Surface Water $CO_2$ and Oxygen Measurements on a Platform in the Central Arkona Sea (Baltic Sea): Seasonality of Uptake and Release. *Mar. Chem.* 101, 220–232. doi: 10.1016/j.marchem.2006.03.004

Lebaron, P., Servais, P., Troussellier, M., Courties, C., Muyzer, G., Bernard, L., et al. (2001). Microbial Community Dynamics in Mediterranean Nutrient-Enriched Seawater Mesocosms: Changes in Abundances, Activity and Composition, FEMS Microbiol. *Ecol* 34, 255–266. doi: 10.1016/S0168-6496(00)00103-3

Lee, J. E., and Kang, J. W. (2020). The Interactive Effects of Elevated Temperature and Nutrient Concentrations on the Physiological Responses of *Ulva linza* Linnaeus (Ulvales, Chlorophyta). *J. Appl. Phycol.* 32, 2459–2467. doi: 10.1007/s10811-019-02031-0

Lee, C.-H., Lee, K., Ko, Y. H., and Lee, J.-S. (2021). Contribution of Marine Phytoplankton and Bacteria to Alkalinity: An Uncharacterized Component. *Geophys. Res. Lett.* 48, e2021GL093738. doi: 10.1029/2021GL093738

Lee, K., Sabine, C. L., Tanhua, T., Kim, T.-W., Feely, R. A., and Kim, H.-C. (2011). Roles of Marginal Seas in Absorbing and Storing Fossil Fuel $CO_2$. *Energy Environ. Sci.* 4, 1133–1146. doi: 10.1039/c0ee00663g

Li, J., Zhang, W., Ding, J., Xue, S., Huo, E., Ma, Z., et al. (2021). Effect of Large-Scale Kelp and Bivalve Farming on Seawater Carbonate System Variations in the Semi-Enclosed Sanggou Bay. *Sci. Total. Environ.* 753, 142065. doi: 10.1016/j.scitotenv.2020.142065

Metzger, J. R., Konar, B., and Edwards, M. S. (2019). Assessing a Macroalgal Foundation Species: Community Variation With Shifting Algal Assemblages. *Mar. Biol.* 166, 156. doi: 10.1007/s00227-019-3606-1

Middelboe, A. L., and Hansen, P. J. (2007). High pH in Shallow-Water Macroalgal Habitats. *Mar. Ecol. Prog. Ser.* 338, 107–117. doi: 10.3354/meps338107

Millero, F. J., Zhang, J. Z., Lee, K., and Campbell, D. M. (1993). Titration Alkalinity of Seawater. *Mar. Chem.* 44, 153–165. doi: 10.1016/0304-4203(93)90200-8

Mineur, F., Arenas, F., Assis, J., Davies, A. J., Engelen, A. H., Fernandes, F., et al. (2015). European Seaweeds Under Pressure: Consequences for Communities and Ecosystem Functioning. *J. Sea. Res.* 98, 91–108. doi: 10.1016/j.seares.2014.11.004

Murie, K. A., and Bourdeau, P. E. (2020). Fragmented Kelp Forest Canopies Retain Their Ability to Alter Local Seawater Chemistry. *Sci. Rep.* 10, 11939. doi: 10.1038/s41598-020-68841-2

Noriega, C., and Araujo, M. (2014). Carbon Dioxide Emissions From Estuaries of Northern and Northeastern Brazil. *Sci. Rep.* 4, 6164. doi: 10.1038/srep06164

Park, G.-H., Lee, K., Tishchenko, P., Min, D.-H., Warner, M. J., Talley, L. D., et al. (2006). Large Accumulation of Anthropogenic $CO_2$ in the East (Japan) Sea and its Significant Impact on Carbonate Chemistry. *Glob. Biogeochem. Cycle.* 20, GB4013. doi: 10.1029/2005gb002676

Pfister, C. A., Altabet, M. A., and Weigel, B. L. (2019). Kelp Beds and Their Local Effects on Seawater Chemistry, Productivity, and Microbial Communities. *Ecology* 100, e02798. doi: 10.1002/ecy.2798

QGIS Development Team (2021) *QGIS Geographic Information System.* Available at: http://qgis.osgeo.org.

Ragazzola, F., Kolzenburg, R., Adani, M., Bordone, A., Cantoni, C., Cerrati, G., et al. (2021). Carbonate Chemistry and Temperature Dynamics in an Alga Dominated Habitat. *Reg. Stud. Mar. Sci.* 44, 101770. doi: 10.1016/j.rsma.2021.101770

Saderne, V., Fusi, M., Thomson, T., Dunne, A., Mahmud, F., Roth, F., et al. (2020). Total Alkalinity Production in a Mangrove Ecosystem Reveals an Overlooked Blue Carbon Component. *Limnol. Oceanogr. Lett.* 6, 61–67. doi: 10.1002/lol2.10170

Sand-Jensen, K., and Nielsen, S. L. (2004). "Estuarine Primary Producers," in *Estuarine Nutrient Cycling: The Influence of Primary Producers. Aquatic Ecology Book Series.* eds. S. L. Nielsen, G. T. Banta and M. F. Pedersen (Dordrecht: Springer), 17–57. doi: 10.1007/978-1-4020-3021-5_2

Semesi, I. S., Beer, S., and Björk, M. (2009). Seagrass Photosynthesis Controls Rates of Calcification and Photosynthesis of Calcareous Macroalgae in a Tropical Seagrass Meadow. *Mar. Ecol. Prog. Ser.* 382, 41–47. doi: 10.3354/meps07973

Shi, X., Zou, D., Hu, S., Mai, G., Ma, Z., and Li, G. (2021). Photosynthetic Characteristics of Three Cohabitated Macroalgae in the Daya Bay, and Their Responses to Temperature Rises. *Plants* 10, 2441. doi: 10.3390/plants10112441

Sippo, J. Z., Maher, D. T., Tait, D. R., Holloway, C., and Santos, I. R. (2016). Are Mangroves Drivers or Buffers of Coastal Acidification? Insights From Alkalinity and Dissolved Inorganic Carbon Export Estimates Across a Latitudinal Transect. *Global Biogeochem. Cycle.* 30, 753–766. doi: 10.1002/2015gb005324

Spector, M., and Edwards, M. S. (2020). Species-Specific Biomass Drives Macroalgal Benthic Primary Production on Temperate Recky Reefs. *Algae* 35, 237–252. doi: 10.4490/algae.2020.35.8.19

Sullaway, G. H., and Edwards, M. S. (2020). Impacts of the non-Native Algal *Sargassum horneri* on Benthic Primary Production in a California Kelp Forest. *Mar. Ecol. Prog. Ser.* 637, 45–57. doi: 10.3354/meps13231

Takeshita, Y., McGillis, W., Briggs, E. M., Carter, A. L., Donham, E. M., Martz, T. R., et al. (2016). Assessment of Net Community Production and Calcification of a Coral Reef Using a Boundary Layer Approach. *J. Geophys. Res. Ocean.* 121, 5655–5671. doi: 10.1002/2016jc011886

Taylor, R., Fletcher, R. L., and Raven, J. A. (2001). Preliminary Studies on the Growth of Selected 'Green Tide' Algae in Laboratory Culture: Effects of Irradiance, Temperature, Salinity and Nutrients on Growth Rate. *Bot. Mar.* 44, 327–336. doi: 10.1515/BOT.2001.042

Turk, D., Yates, K. K., Vega-Rodriguez, M., Toro-Farmer, G., L'Esperance, C., Melo, N., et al. (2015). Community Metabolism in Shallow Coral Reef and Seagrass Ecosystems, Lower Florida Keys. *Mar. Ecol. Prog. Ser.* 538, 35–52. doi: 10.3354/meps11385

Vachon, D., Sadro, S., Bogard, M. J., Lapierre, J.-F., Baulch, H. M., Rusak, J. A., et al. (2020). Paired $O_2$-$CO_2$ Measurements Provide Emergent Insights Into Aquatic Ecosystem Function. *Limnol. Oceanogr. Lett.* 5, 287–294. doi: 10.1002/lol2.10135

Wahl, M., Schneider Covachã, S., Saderne, V., Hiebenthal, C., Müller, J. D., Pansch, C., et al. (2018). Macroalgae may Mitigate Ocean Acidification Effects on Mussel Calcification by Increasing pH and its Fluctuations. *Limnol. Oceanogr.* 63, 3–21. doi: 10.1002/lno.10608

Weigel, B. L., and Pfister, C. A. (2019). Successional Dynamics and Seascape-Level Patterns of Microbial Communities on the Canopy-Forming Kelps *Nereocystis luetkeana* and *Macrocystis pyrifera*. *Front. Microbiol.* 10, 346. doi: 10.3389/fmicb.2019.00346

Xiao, X., Agusti, S., Yu, Y., Huang, Y., Chen, W., Hu, J., et al. (2021). Seaweed Farms Provide Refugia From Ocean Acidification. *Sci. Total. Environ.* 776, 145192. doi: 10.1016/j.scitotenv.2021.145192

Yoo, J. S., Park, I. S., Song, Y. C., Seo, Y. W., Doe, G. Y., Lee, J. W., et al. (2006). Characteristics and Structure of Benthic Algal Community in Pohang New Port Area. *J. Navig. Port. Res.* 30, 309–314. doi: 10.5394/KINPR.2006.30.4.309

Zhai, W., and Dai, M. (2009). On the Seasonal Variation of Air – Sea $CO_2$ Fluxes in the Outer Changjiang (Yangtze River) Estuary, East China Sea. *Mar. Chem.* 117, 2–10. doi: 10.1016/j.marchem.2009.02.008

Zhai, W. D., Dai, M., and Cai, W. J. (2009). Coupling of Surface $p$CO$_2$ and Dissolved Oxygen in the Northern South China Sea: Impacts of Contrasting Coastal Processes. *Biogeosciences* 6, 2589–2598. doi: 10.5194/bg-6-2589-2009

Zhao, X., Zhong, Y., Zhang, H., Qu, T., Hou, C., Guan, C., et al. (2021). Comparison of Environmental Responding Strategies Between *Ulva prolifera* and *Sargassum horneri*: An *In-Situ* Study During the Co-Occurrence of Green Tides and Golden Tides in the Yellow Sea, China in 2017. *J. Oceanol. Limnol.* 39, 2252–2266. doi: 10.1007/s00343-021-0397-2

**Conflict of Interest:** The authors declare that the research was conducted in the absence of any commercial or financial relationships that could be construed as a potential conflict of interest.